Journal of Hydrology 639 (2024) 131632

Contents lists available at ScienceDirect

Journal of Hydrology

journal homepage: www.elsevier.com/locate/jhydrol

Research papers

A simple mixing model using electrical conductivity yields robust hydrograph separation in a tropical montane catchment

Patricio X. Lazo [a,b], Giovanny M. Mosquera [c], Irene Cárdenas [a], Catalina Segura [d], Patricio Crespo [a,b,*]

[a] Departamento de Recursos Hídricos y Ciencias Ambientales, Universidad de Cuenca, Av. 12 de Abril, Cuenca, Ecuador
[b] Facultad de Ingeniería, Universidad de Cuenca, Av. 12 de Abril, Cuenca, Ecuador
[c] Departamento de Ingeniería & Grupo de Glaciología y Ecohidrología de Montañas Andinas (GEMS), Pontificia Universidad Católica del Perú (PUCP), Lima, Perú
[d] Department of Forest Engineering, Resources, and Management, Oregon State University, Corvallis, OR, USA

ARTICLE INFO

This manuscript was handled by Marco Borga, Editor-in-Chief, with the assistance of Francesco Comiti, Associate Editor?

Keywords:
tropical Andes
Páramo
Flow partition
Specific conductance
TraSPAN
Mixing model

ABSTRACT

Hydrograph separation assessment is crucial to understand stormflow generation at catchments worldwide. Tracer-based methods provide robust estimations of event (or new) and pre-event (or old) water fractions as they account for external and internal catchment hydrological behavior. While models of different mathematical and computational complexity are often used in tracer-based hydrograph separation studies, direct comparisons between those models are limited. Here, we compare hydrograph separation results yielded by the simplest Two-Component Mixing Model (TCMM) and a Tracer-based Streamflow Partitioning ANalysis model (TraSPAN) assumed to provide robust results as it combines conceptual rainfall-runoff modelling with tracers' mass balance. We carried out the analysis using high temporal frequency (sub-daily to sub-hourly) data of two tracers, Oxygen-18 and Electrical Conductivity (EC), monitored during 37 rainfall-runoff events with different hydrometeorological conditions in a high-Andean páramo catchment located at the Zhurucay Ecohydrological Observatory in southern Ecuador. Both approaches yield similar estimations of event and pre-event water fractions regardless of the tracer used as long as appropriate concentrations of event (C_e) and pre-event (C_p) water for the TCMM are determined. Although the estimate of C_e has little influence with one rainfall sample collected during the event being sufficient to obtain reliable results, results hinge heavily on the estimate of C_p. We found that the TCMM yields similar results than TraSPAN when C_p is represented by the stream water concentration corresponding to a sample collected prior to the beginning of each of the events. We conclude that the combination of a simple framework (TCMM) with sub-hourly EC measurements provides reliable hydrograph separation results when representative C_p samples are used. These findings will allow to lower the logistical and economical resources needed to adequately assess hydrograph separation and to carry out quasi-continuous assessments of flow partitioning with high accuracy in high-Andean páramo catchments.

1. Introduction

Understanding the hydrological processes involved in runoff generation remains challenging given climatological and biophysical differences among catchments worldwide. Flow partitioning modelling is an approach often used to understand how precipitation mixes with different subsurface water storages (i.e., streams, soils, groundwater; Shope, 2016), and to determine the contribution of different water sources to streams at different time scales (McGlynn et al., 2004). This approach has helped to delineate water flow paths (e.g., Goller et al., 2005; Klaus and McDonnell, 2013), conceptualize runoff generation processes (e.g., Camacho Suarez et al., 2015; Mosquera et al., 2018; Muñoz-Villers and McDonnell, 2012; Sklash and Farvolden, 1979; Soulsby et al., 2011; Tetzlaff et al., 2015a), identify thresholds in runoff generation (e.g., Detty and McGuire, 2010; Litt et al., 2015), and estimate water travel times (e.g., Harman, 2015; Lee et al., 2020; McGuire and McDonnell, 2006; Soulsby et al., 2015).

Determining the amount of event (or new) and pre-event (or old)

* Corresponding author.
E-mail addresses: gmosquerar@pucp.edu.pe (G.M. Mosquera), irene.cardenas@ucuenca.edu.ec (I. Cárdenas), Catalina.Segura@oregonstate.edu (C. Segura), patricio.crespo@ucuenca.edu.ec (P. Crespo).

https://doi.org/10.1016/j.jhydrol.2024.131632
Received 27 October 2023; Received in revised form 24 May 2024; Accepted 16 June 2024
Available online 2 July 2024

water contributing to streamflow using tracer-based techniques is one of the most used flow partitioning analysis in hydrological research (Pelletier and Andréassian, 2020; Cartwright and Morgenstern, 2018; Tetzlaff et al., 2015b). These methods allow defining catchment internal flow paths and storages (Stadnyk et al., 2013) that cannot be identified based on streamflow data alone (Beven and Binley, 1992; Dunn et al., 2008; Fenicia et al., 2008; Seibert and McDonnell, 2002). Two Component Mixing Model (TCMM) and Tracer-Aided Rainfall-Runoff Models (TARRM) have been used in catchments worldwide (Birkel and Soulsby, 2015; Klaus and McDonnell, 2013). The TCMM is a mass balance approach that has been used for over the last 40 years (Pinder and Jones, 1969; Sklash and Farvolden, 1979). The TARRM combine conceptual rainfall-runoff models with tracers and has been around for 20 years (Birkel et al., 2014, 2010; Delavau et al., 2017; Lazo et al., 2023; Mosquera et al., 2018; Smith et al., 2016; Tetzlaff et al., 2008; Weiler et al., 2005). Although both approaches yield event-based estimates of new and old water there are few comparisons of their performance (i.e., Lyon et al., 2008).

Despite which type of tracer-based model is selected, the sources (i.e., new and old water) concentrations must be well defined to adequately asses flow partitioning results (Liu et al., 2004). In this sense, several authors have addressed the subject and proposed different strategies to determine these concentrations. In terms of event water source concentration, rainfall is often accepted as the main contributor of new water to streamflow with a bulk rainfall sample often assumed as representative of the entire event component (Bansah and Ali, 2017; Klaus and McDonnell, 2013). However, McDonnell et al. (1990) proposed three methods to determine the concentration of new water source by transforming the concentrations of all samples collected during individual rainfall-runoff events into one using: i) a weighted mean, ii) an incremental mean, and iii) an incremental intensity mean. They determined that alternatives ii) and iii) were more effective as they overcome the problem presented by bulk samples in which old water estimates at any point before the end of the event will be influenced by rain that has not yet entered the catchment, making the assumption physically incorrect.

Old water source concentration is often characterized as the concentration of tracer samples collected from the stream at baseflow (e.g., Blume et al., 2008; Litt et al., 2015; Obradovic and Sklash, 1986; Pinder and Jones, 1969) assuming that at this stage only pre-event water contributes to the streamflow. The tracer signal of stream water samples collected prior to the beginning of the event is also frequently selected as pre-event water source (e.g., McDonnell et al., 1990; Pellerin et al., 2008; Sklash and Farvolden, 1979; von Freyberg et al., 2018, 2017) assuming that pre-event water comes from a fully mixed reservoir (Lyon et al., 2008). Other studies have used the average tracer concentration in stream samples collected at low flow (e.g., Obradovic and Sklash, 1986; Onda et al., 2006), or in samples collected at groundwater wells (Iwagami et al., 2010). However, it remains unclear which of these concentrations is most adequate for different catchments around the world. This situation highlights how challenging it is to determine pre-event concentration due to its spatial and temporal variability that could affect flow partitioning results. It is also worth noting that most studies assessing different event and pre-event water concentrations in flow partitioning have been mainly conducted in forested, glacial, and temperate environments, highlighting the need to carry out investigations in other understudied regions such as the tropics.

Due to the conservative behavior of water stable isotope ratios (Kendall and McDonnell, 1998), they are widely used as tracer to perform event and pre-event flow partitioning. Although technology has enable high-resolution sampling of water for H^2 and ^{18}O analysis, it is still a major challenge to maintain this type of monitoring setups for long term (Birkel and Soulsby, 2015). Thus, several alternative tracers have been tested in flow partitioning studies including electrical conductivity (EC; e.g.,Cano-Paoli et al., 2019; Cey et al., 1998; Correa et al., 2019; Laudon and Slaymaker, 1997; Lazo et al., 2023; Mosquera et al., 2018; Pellerin et al., 2008), chloride (e.g., Brown et al., 1999; Leaney et al., 1993; Monteith et al., 2006; Turner et al., 1987), silica (e.g., Durand et al., 1993; Hooper and Shoemaker, 1986; Munyaneza et al., 2012; Nolan and Hill, 1990), alkalinity (e.g., Ribolzi et al., 1996), sodium (e.g., Pionke et al., 1993; Suecker et al., 2000) and calcium (Johnson et al., 2023). Among them, approaches using EC have provided similar flow partitioning results in different settings including alpine forested and grasslands (e.g., Cano-Paoli et al., 2019; Laudon and Slaymaker, 1997), mediterranean forested (Mosquera et al., 2018), subtropical semi-arid grasslands (e.g., Camacho Suarez et al., 2015), temperate tile-drained (Vidon and Cuadra, 2010), tropical urban glaciated (e.g., Meriano et al., 2011), and tropical montane grasslands (Lazo et al., 2023). The use of EC allows higher tracer resolution at a lower cost than water stable isotope ratios. EC in the context of TCMM could help reduce uncertainty and calculation time when dealing with large datasets. In addition, this could facilitate the selection of event and pre-event end-members concentrations given the large amount of information available, resulting in more accurate estimations that benefits the analysis of process thresholds and short term catchment processes (Floury et al., 2017; Sahraei et al., 2020; Stockinger et al., 2016).

In this study, we use a high temporal frequency sampling scheme deployed at a tropical montane ecosystem to monitor hydrometric and tracer data during 37 rainfall-runoff events with the following objectives: i) to test how the selection of different event and pre-event water source concentrations influences flow partitioning results using EC and ^{18}O, ii) to examine if models of different complexity yield similar flow partitioning results, and iii) to compare flow partitioning modelling results using EC and ^{18}O.

2. Materials and methods

2.1. Study site

The study site is a tropical páramo catchment located within the Zhurucay Ecohydrological Observatory (ZEO) in southern Ecuador (3°04′S, 79°14′W). The catchment has a drainage area of 3.28 km^2 and extends between 3,680 to 3,900 m a.s.l. (Fig. 1). Climate is mainly influenced by air masses stemming from east flank of the Andean cordillera through the Amazon rainforest (Esquivel-Hernández et al., 2019; Zhiña et al., 2022). Mean annual precipitation (±standard deviation) at 3,780 m a.s.l. during the period 2011–2018 was 1222 ± 22 mm (Larco et al., 2023). Precipitation is mainly delivered as low intensity rainfall events (<5 mm/hr) that falls all year round as drizzle (Padrón et al., 2015). This nearly constant precipitation input in combination with the high porosity and hydraulic conductivity of the soils results in a flashy streamflow response to precipitation (Mosquera et al., 2015; Mosquera et al., 2016a), where shallow subsurface flow through the little developed soils (up to 1 m depth) is dominant (Mosquera et al., 2016b). Annual evapotranspiration is relatively low (610 mm on average during the period 2016–2019) (Ochoa-Sánchez et al., 2020) as a result of low mean annual temperature (6.3 ± 1.24 °C) and high relative humidity (92.3 ± 8.3 %) at 3,780 m.a.s.l. (Larco et al., 2023).

The site is underlied by the Quimsacocha and Turi formations. The Quimsacocha formation consists of basaltic flows with plagioclases, feldspars, and andesitic pyroclastics. The Turi formations is dominated by tuffaceos andesitic breccias, conglomerates, and horizontal stratified sands. Both formations have very low permeability (Zuñiga, 2018). Dominant soils are Andosols and Histosols (IUSS Working Group WRB, 2015) originated from the accumulation of volcanic ash and organic matter. As a result, these soils are humic, acid, and present a high water retention capacity (Mosquera et al., 2021; Quichimbo et al., 2012). Vegetation cover is mainly composed of tussock grasses (*Calamagrostis* sp.) overlying Andosol soil at hillslope positions and covering 71 % of the catchment area. Cushion plants (*Plantago rigida, Xenophyllum humile, Azorella* spp.) overlying the Histosols are found at flat areas, mainly valley bottoms, and represent 24 % of the catchment area. Native forests

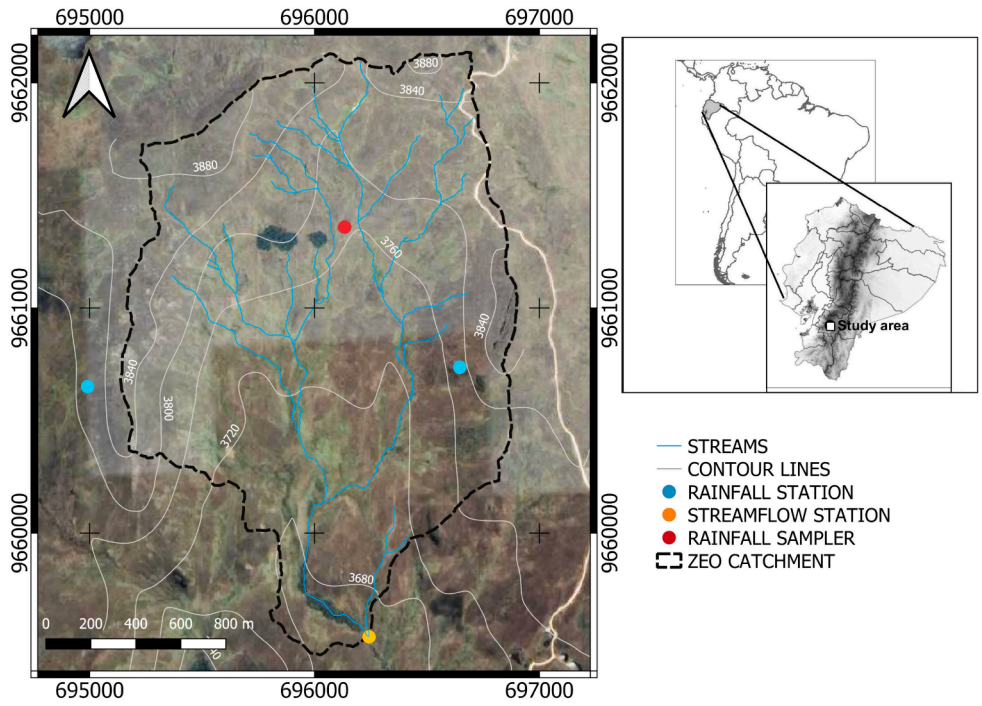

Fig. 1. Location of precipitation and hydrometric stations situated at the Zhurucay Ecohydrological Observatory (ZEO) in south Ecuador.

(*Polylepis reticulata*) and pine plantations (*Pinus patula*) cover less than 5 % of the land. Land use practices in the catchment are limited to light grazing mainly at lower elevations (Mosquera et al., 2015).

2.2. Hydrometric data collection

Precipitation and water level data were collected from October-2017 to June-2019. We used four HOBO (RG3-M, Onset Computer Corporation, Bourne, MA, USA) rain gauge tipping buckets (0.2 mm resolution) distributed across the catchment to measure precipitation (Fig. 1) (Lazo et al., 2019). Water level at the catchment outlet was recorded every 5 min with a INW pressure transducer (AquiStar CT2X, Kirkland, WA, USA) placed in a V-notch weir. Streamflow values were calculated from water level data using the Kindsvater-Shen equations (U.S. Bureau of Reclamation, 2001), and these equations were calibrated using the constant rate salt dilution method (Guallpa et al., 2022).

2.3. Tracer data collection

Water samples for ^{18}O analysis were collected from October-2017 to June-2019. Rainfall samples were collected using a volumetric sequential rainfall sampler located at the upper part of the catchment (Fig. 1). The collector was free from evaporative effects (Lazo et al., 2023; Zhiña et al., 2022). Streamwater samples were collected using a PVS4120D autosampler (Campbell Scientific, Logan, UT, USA) at different sampling intervals. From October-2017 to January-2018 samples were collected every 6 h, from January-2018 to March-2019 the sampling interval was every 4 h, and from March-2019 to June-2019 samples were collected hourly. Streamwater samples were filtered using 0.45 μm polypropylene single-use syringe membrane filters (Puradisc 25 PP Whatman Inc., Clifton, NJ, USA). All water samples were stored in 2 ml amber glass bottles, sealed with parafilm, and kept away from sunlight to prevent fractionation.

A cavity ring-down spectrometer (Picarro 2130-I; Picarro Inc., USA) was used to measure oxygen-18 isotopic composition. Precipitation and streamwater samples were analyzed in separate runs to reduce memory effects (Penna et al., 2012).

EC was manually measured in rainfall samples collected from the volumetric sequential rainfall sampler. A WTW Universal Multi-Parameter (Handheld ProfiLine Multi 3320, Xylem Analytics Germany GmbH, Weilheim, Germany) equipped with a conductivity measuring cell (TetraCon 325, Xylem Analytics Germany GmbH, Weilheim, Germany) was used to measure EC in rainfall samples (accuracy of ± 0.5 % of the measured value). This equipment was calibrated for each sampling campaign (i.e., every 5 days/weeks). Stream water EC was continuously recorded at the catchment outlet using the same probe that measured water level (i.e., INW CT2X, accuracy of ± 0.5 % of the measured EC value) at a 5-minute resolution. The calibration of the probe was carried out before installation and every 6 months afterwards. Rainfall and streamflow EC data are reported in μS/cm.

2.4. Rainfall-runoff events selection

Rainfall-runoff events were defined using the Peak Over Threshold approach (POT; Lang et al., 1999), which selects all peak values above a streamflow threshold. In this study, the threshold was defined as the Q_{35} non-exceedance flow rate that corresponds to low flow values for the ZEO (Mosquera et al., 2015). Therefore, every runoff response to rainfall that started below this threshold and reached peak flow above it was considered as a rainfall-runoff event. Because of the frequent occurrence of rainfall at the ZEO (Padrón et al., 2015), a time of 6 h was selected as the minimum inter-event criteria (Dunkerley, 2008) to account also for precipitation dynamic. R software version 3.5.1 with the POT package (Ribatet and Dutang, 2004) was used for the analysis.

In order to characterize all the monitored events and evaluate the flow conditions in which flow partitioning was performed; several hydrological variables were estimated. These variables included event duration, peak flow, cumulative rainfall, cumulative streamflow, average rainfall intensity, average streamflow, and runoff coefficient. The latter was estimated as cumulative streamflow to cumulative rainfall for each of the events.

2.5. Flow partitioning modelling

Flow partitioning modelling for all the events was conducted using the two approaches described below.

2.5.1. Two component mixing model (TCMM)

The two component hydrograph separation proposed by Pinder and Jones (1969) was used to estimate the event and pre-event water fractions forming streamflow during events, where the required assumptions proposed in Pearce et al. (1986) and Sklash et al. (1986) were met. The following mass-balance equations were used for calculation:

$$Q_t = Q_e + Q_p \tag{1}$$

$$C_t Q_t = C_e Q_e + C_p Q_p \tag{2}$$

where Q is streamflow, C refers to the tracer concentration, and the subscripts t, e, and p refer to total, event, and pre-event, respectively.

Equations (1) and (2) were combined to determine the pre-event water fraction (F_p):

$$F_p = \frac{C_s - C_e}{C_p - C_e} \tag{3}$$

Uncertainty in the TCMM results was estimated following the Gaussian standard error method proposed by Genereux (1998):

$$W_{fp} = \sqrt{\left[\frac{f_p}{(C_e - C_p)} W_{C_p}\right]^2 + \left[\frac{f_e}{(C_e - C_p)} W_{C_e}\right]^2 + \left[\frac{-1}{(C_e - C_p)} W_{C_t}\right]^2}$$

where W is uncertainty, C is the tracer concentration, f is the mixing fraction and the subscripts e, p, t refers to the event, pre-event, and total stream water components. Analytical errors were assumed as 0.1 ‰ for $\delta^{18}O$ and 5 % of the measured value for EC.

2.5.2. Tracer-aided rainfall-runoff model (TARRM)

The Tracer-based Streamflow Partitioning Analysis model (TraSPAN; Mosquera et al., 2018; Segura et al., 2012) was also used for the estimation of the event and pre-event water fractions to streamflow. This tracer-aided rainfall-runoff model is based on the unit hydrograph to account for streamflow response to rainfall events, in combination with transit time distributions (TTDs) to simulate catchment internal mixing processes through tracer mass balance. The model is composed of three modules. The first module estimates effective rainfall (P_{eff}) as the product of antecedent rainfall index (Jakeman and Hornberger, 1993) and precipitation. Module 2 calculates the fraction of P_{eff} routed as event or pre-event water and module 3 computes the event (Q_e) and pre-event (Q_p) water fractions by solving the convolution of the TTDs. The estimation of the tracer concentration is obtained by combining the convolution results with the mass balance approach. A detailed description of the model is presented in Mosquera et al. (2018).

Although the model allows setting up different structures representing different catchment hydrological behavior, here we report results of the structure that best represents the rainfall-runoff response at the ZEO determined by Lazo et al. (2023). As such, we assume that the fraction of P_{eff} routed as event water is time-variant and that water is routed in a Two Parallel Linear Reservoirs TTD. A representation of the model structure and the main equations are presented in Figure S1 and Table S1.

Model calibration was carried out through a Monte Carlo approach. The model was run 1,000,000 times for each event to randomly define a set of parameters for each simulation (Beven and Freer, 2001). The goodness of fit of the model simulations was assessed using the Kling-Gupta Efficiency (KGE; Gupta et al., 2009) metric by comparing the modelled runoff and tracer signals to the observed data. The "best" event and pre-event water source concentrations in our model framework were numerically defined by obtaining the combination of C_e and C_p that yielded the highest KGE values. For C_e, we considered three alternatives weighted mean, an incremental mean, and an incremental intensity mean (McDonnell et al., 1990), C_p was included as a model parameter in the Monte Carlo approach to asses a range of possible C_p values. This range was defined by the values of the streamwater concentrations prior to each of the 37 events, and the value of the concentration measured at baseflow for each tracer (i.e., tracer concentrations of stream water samples collected at flow below the 5th percentile of the non-exceedance flow rate curve). Therefore, the selected C_e and C_p source concentrations and flow partitioning results obtained using this TraSPAN structure were assumed as the basis for comparison with those yielded by the TCMM.

2.6. Selection of event and pre-event water samples

We tested different combinations of C_e and C_p for the two-component mixing model. In terms of C_e, we analyzed six different possibilities (E1 to E6; Table 1) that included: (i) the precipitation concentrations of the samples according to the time that they were taken during the rainfall-runoff event (E1), (ii) the incremental mean technique (E2; McDonnell et al., 1990), (iii) volume weighted average (E3; McDonnell et al., 1990), (iv) the first precipitation sample collected during the event (E4), (v) the

Table 1
List of event (E) and pre-event (PE) water samples used for flow partitioning modelling in this study.

Code	Description	Reference
PE1	Pre-event concentration corresponding to the streamflow sample taken before the start of the event.	(McDonnell et al., 1990; Pellerin et al., 2008a; Sklash and Farvolden, 1979)
PE2	Pre-event concentration corresponding to the average of the three streamflow samples taken prior to the event.	(Bonell et al., 1990; von Freyberg et al., 2018, 2017)
PE3	Pre-event concentration corresponding to the average of the streamflow samples taken during the lowest flows (below 35th percentile of the non-exceedance flow rate curve) of the year in which the event occurred	(Obradovic and Sklash, 1986)
PE4	Pre-event concentration corresponding to the average of the streamflow samples taken during the lowest flows (below 35th percentile of the non-exceedance flow rate curve) of the last 6 years	(Obradovic and Sklash, 1986; Onda et al., 2006)
PE5	Pre-event concentration corresponding to the average of the streamflow samples taken during the baseflow (based on the recession constant) of the year in which the event occurred	(Litt et al., 2015; Obradovic and Sklash, 1986; Pinder and Jones, 1969)
PE6	Pre-event concentration corresponding to the average of the streamflow samples taken during the baseflow (based on the recession constant) of the last 6 years	(Litt et al., 2015; Obradovic and Sklash, 1986; Pinder and Jones, 1969)
E1	Precipitation concentrations of the samples according to the time that they were taken during the rainfall-runoff event	*
E2	Event concentration corresponding to the cumulative incremental weighted mean of the precipitation samples taken during the event.	(McDonnell et al., 1990)
E3	Event concentration corresponding to the standard weighted mean of the precipitation samples taken during the event.	(McDonnell et al., 1990)
E4	Event concentration corresponding to the first precipitation sample taken during the event.	*
E5	Event concentration corresponding to the last precipitation sample taken during the event.	(Bansah and Ali, 2017)
E6	Event concentration corresponding to the precipitation sample taken at the peak of precipitation during the event.	*

* Codes without reference are the ones proposed by the authors of this study.

last precipitation sample taken during the event (E5; Bansah and Ali, 2017), and (vi) the precipitation sample corresponding to the tracer concentration peak (E6).

We also considered six C_p options, two based on antecedent rainfall conditions-related (PE1-PE2) and four base flow-related (PE3-PE6). PE1 was equal to the concentration of the stream sample collected immediately before the rain event started while PE2 was the average of the three stream samples collected prior to the rain event. The base flow C_p definitions PE3 was defined as the average of the concentrations of stream samples collected at the flow below the Q_{35} (non-exceedance 35th percentile in the flow rate curve; Mosquera et al., 2015; Smakhtin, 2001) at the year of the event, whereas PE4 is the same as PE3 but using the concentrations from the last 6 years. PE5 was defined as the average concentrations from stream samples collected at base flow (i.e., based on the recession constant, mainly below 5th percentile of the non-exceedance flow rate curve) at the year of the event and PE6 is the same as PE5 but with the concentrations of the last 6 years. Base flow values were calculated using the WETSPRO(Willems, 2009).

2.7. Statistical analysis

We performed a Pearson linear correlation analysis among the hydrometric variables mentioned in section 2.4 at a significant level of 0.05 ($\alpha = 0.05$).

A multiple pairwise comparison using the Nemenyi's test (Hollander et al., 2013) at a significance level of 0.05 ($\alpha = 0.05$) was carried out to compare the results obtained by using different samples representing C_e and C_p, different flow partitioning models (TCMM versus TARRM), and different tracers ($\delta^{18}O$ versus EC), thus; a p-value lower than 0.05 means that the differences are significant. This procedure was carried out in three steps: (i) we compared the results obtained from the TCMM using different C_e and C_p combinations for each tracer ($\delta^{18}O$ and EC) independently; (ii) we compared the results obtained by the TCMM with the results obtained by the TARRM (i.e., TraSPAN model); and (iii) we compared the results yielded by $\delta^{18}O$ and EC using the TCMM.

3. Results

3.1. Rainfall-runoff events characterization

Thirty-seven rainstorm events were monitored during the study period. The events presented a wide range of magnitude (0.0016–0.1786 mm) and durations varying (10–104 h). Events lasting longer than 70 h ($n = 3$) generally produced low peak flow values. The rest of the events lasted less than 52 h regardless of their peak flow value (Table 2). Cumulative rainfall volume for the events ranged between 2.9 and 26.2 mm, presenting a variable average rainfall intensity ranging between 0.1 (Event 1) and 0.8 mm/h (Event 26). Streamflow presented a cumulative volume ranging between 0.55 (Event 1) and 22.65 mm (Event 37), and the average event streamflow varied between 0.01 (Event 1) and 0.76 mm/h (Event 37). The event's runoff coefficient covered a wide range with a minimum value of 0.05 (Event 1) and a maximum value of 0.92 (Event 20). None of the evaluated variables were correlated with peak flow.

Table 2
Hydrometeorological characteristics and number of samples collected at the 37 rainfall-runoff events monitored in this study.

Event code	Duration (hour)	Peak flow (mm)	Cumulative rainfall (mm)	Cumulative streamflow (mm)	Average rainfall intensity (mm/hr)	Average streamflow (mm/hr)	Runoff coefficient	Number of Samples	
								Streamflow	Precipitation
1	96.00	0.0016	10.3	0.55	0.1	0.006	0.05	17	3
2	104.00	0.0022	13.9	1.00	0.1	0.010	0.07	15	4
3	103.00	0.0027	12.8	1.28	0.1	0.012	0.10	26	4
4	89.00	0.0031	15.2	1.57	0.1	0.018	0.10	15	6
5	29.17	0.0133	5.9	2.74	0.2	0.094	0.46	25	4
6	16.67	0.0134	6.7	2.05	0.4	0.123	0.31	15	5
7	33.33	0.0136	6.9	3.47	0.2	0.104	0.50	17	2
8	25.00	0.0139	5.2	2.41	0.2	0.096	0.46	3	2
9	28.00	0.0150	6.0	2.12	0.2	0.076	0.35	5	2
10	18.33	0.0160	9.1	1.88	0.5	0.103	0.21	5	2
11	21.67	0.0177	8.7	2.37	0.4	0.109	0.27	16	4
12	21.67	0.0182	6.1	3.21	0.2	0.148	0.53	5	3
13	33.33	0.0182	11.0	3.50	0.3	0.105	0.32	7	2
14	30.00	0.0185	8.8	4.35	0.3	0.145	0.49	6	4
15	31.00	0.0186	10.5	4.16	0.3	0.134	0.40	6	6
16	25.00	0.0199	8.6	1.97	0.3	0.079	0.23	7	3
17	16.67	0.0205	2.9	2.58	0.1	0.155	0.88	5	2
18	24.00	0.0205	8.1	2.83	0.3	0.118	0.35	6	2
19	29.17	0.0222	8.3	3.28	0.2	0.112	0.39	9	6
20	20.00	0.0247	3.4	3.20	0.1	0.160	0.92	20	2
21	70.00	0.0271	16.6	7.97	0.2	0.114	0.48	18	6
22	20.83	0.0282	10.2	3.33	0.4	0.160	0.33	6	2
23	52.00	0.0336	8.9	6.37	0.1	0.123	0.72	12	3
24	18.33	0.0410	9.4	4.44	0.5	0.242	0.47	6	3
25	29.17	0.0458	12.1	5.85	0.4	0.201	0.48	8	4
26	24.00	0.0472	21.4	3.73	0.8	0.155	0.17	4	6
27	23.00	0.0479	13.6	3.75	0.5	0.163	0.27	5	4
28	28.33	0.0499	9.0	6.89	0.3	0.243	0.77	7	4
29	10.00	0.0502	7.3	3.77	0.7	0.377	0.52	7	5
30	20.83	0.0527	8.3	5.44	0.4	0.261	0.65	18	5
31	25.00	0.0608	12.4	7.05	0.5	0.282	0.57	7	3
32	14.17	0.0664	11.4	6.77	0.8	0.478	0.59	9	9
33	43.00	0.0859	21.5	11.07	0.5	0.257	0.51	4	9
34	25.00	0.1150	16.0	14.13	0.6	0.565	0.88	7	3
35	24.00	0.1216	12.3	9.51	0.5	0.396	0.77	5	5
36	25.00	0.1324	15.7	8.52	0.6	0.341	0.54	5	5
37	30.00	0.1786	26.2	22.65	0.8	0.755	0.86	8	5

3.2. High-resolution tracer monitoring

Isotopic data monitored from October-2017 to June-2019 showed that $\delta^{18}O$ rainfall concentrations presented an average of −12.3 ‰ ranging between −2.4 ‰ to −27.9 ‰. The lowest isotopic values were observed during the most humid periods (April to June), whereas the highest values occurred in February and from June to October (Fig. 2a). Despite the large range of variation in the isotopic composition of rainfall during the study period (25.4 ‰), the variation at event scale was much smaller ranging from 3.5 ‰ to 0.8 ‰. Runoff $\delta^{18}O$ concentrations showed an average of −10.7 ‰ and ranged from −7.6 ‰ to −15.5 ‰ following a similar temporal variation than rainfall isotopic composition.

EC in rainfall had an average of 8 µS/cm within a range of 20 µS/cm and 1 µS/cm during the study period. The highest values were generally observed in February, April, and May; while the lowest values were recorded in July and August (Fig. 2b). Similar to $\delta^{18}O$ rainfall observations, the variability of rainfall EC during rainfall events was much smaller (2.5 +/- 1.2 µS/cm) than the variation found during the whole study period (19 +/- 10.4 µS/cm. EC in runoff averaged 34.6 µS/cm, ranging between 66.5 and 11.8 µS/cm, with the highest values observed from September to November and the lowest values during February and March.

3.3. Flow partitioning using TCMM with different combinations of event and pre-event water tracer input data

For each tracer ($\delta^{18}O$ and EC) a total of 36 different combinations of event (C_e; E1 to E6) and pre-event (C_p; PE1 to PE6) tracer input data were used to perform the hydrograph separation using the TCMM for the 37 monitored events.

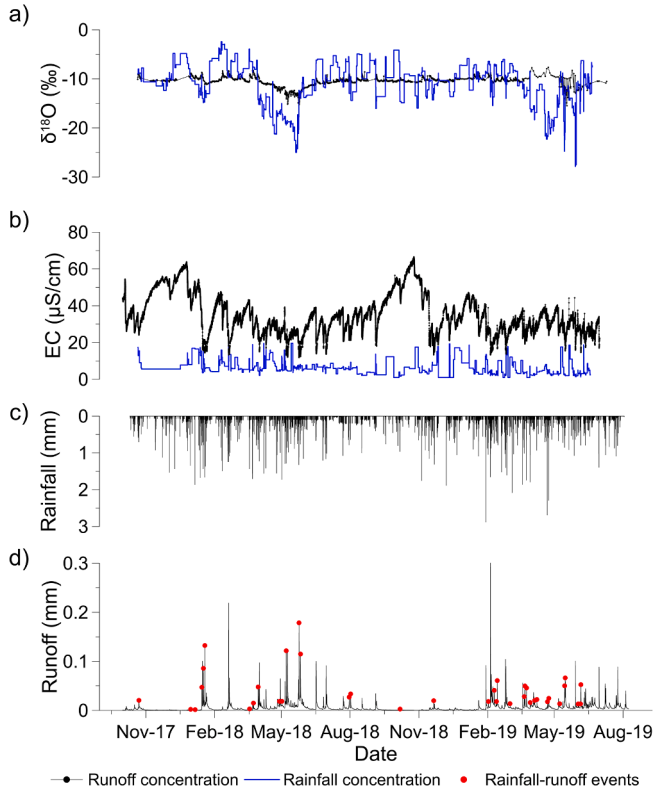

Fig. 2. Time series of the sub-daily a) isotopic composition of $\delta^{18}O$ and b) electrical conductivity (EC) in rainfall (red line) and streamflow (black dotted line), c) daily rainfall, and d) daily streamflow at the Zhurucay Ecohydrological Observatory during the period October 2017-June 2019. Red dots in d) indicate the 37 rainfall-runoff events monitored and used for hydrograph separation in this study. (For interpretation of the references to color in this figure legend, the reader is referred to the web version of this article.)

When using $\delta^{18}O$ the medians of the pre-event water fractions were above 80 % for all the combinations (Fig. 3). The interquartile ranges of the pre-event water fractions varied between 82 and 100 % when using PE1 and PE2 regardless of the C_e value used, and were larger when using PE3, PE4, PE5, and PE6 (60–100 %). All C_e values (E1 to E6) yielded similar pre-event water fractions (median and interquartile range) for each C_p value (Fig. 3). These differences were lower than 5 % when using PE1 and PE2 (Fig. 3a and 3b) and higher than 5 % but lower than 10 % for PE3, PE4, PE5, and PE6 (Fig. 3c, 3d, 3e, and 3f). In terms of minimum of the pre-event water fraction values, PE1 and PE2 showed a large variation depending on the C_e used, with differences higher than 20 % among the six different Ce definitions (Fig. 3a and 3b). When using PE3, PE4, PE5, and PE6, the minimum values of pre-event water fraction were 0 % for all the combinations. The maximum values of pre-event water fraction were 100 % for all cases. All p-values of the statistical test were higher than 0.05 (Fig. 4), meaning that no significant differences were found between pre-event water fractions estimates when using different combinations of C_p and C_e values.

When using EC as the tracer in the TCMM and regardless of the C_e value used, the medians of the pre-event water fractions fluctuated between 80 and 90 % for PE1 and PE2 (Fig. 5a and 5b), higher than 50 % but lower than 60 % for PE3 and PE4 (Fig. 5c and 5d), and around 45 % for PE5 and PE6 (Fig. 5e and 5f). Small differences (<5%) in the median and interquartile ranges of the pre-event water fractions were observed for different C_e values (E1, E2, E3, E4, E5, and E6) for each of the C_p values (PE1, PE2, PE3, PE4, PE5, and PE6; Fig. 5). When comparing the minimum values of pre-event water fraction, PE1 presented the lowest difference when using E1 and E2 as C_e; whereas models using PE3, PE4, PE5, and PE6 resulted in minimum values of pre-event water fraction close or equal to 0 % (Fig. 5). Maximum values of pre-event water fraction for all the combinations where around 100 %. In addition, p-values of the statistical test show that combinations including PE5 and PE6 present significant differences (i.e., $p < 0.05$) in relation to those using PE1, PE2, PE3 as C_p.

3.4. Comparison of flow partitioning models of different complexity

The C_e-C_p combinations in the TCMM presenting the most similar pre-event water fractions in comparison to TraSPAN (TARRM) results were PE1 with E1 and E2 when using $\delta^{18}O$. These combinations presented differences lower than 5 % for the maximum values and lower than 10 % for PE1-E1 and lower than 15 % for PE1-E2 when considering minimum pre-event water fraction values (Fig. 3a). Differences lower than 5 % were also observed for the interquartile ranges of the pre-event water fractions using the aforementioned combinations in relation to TrasPAN results (Fig. 3a). Other C_e-C_p combinations presented larger differences compared to TrasPAN, normally higher than 15 % for maximum, minimum, median, and interquartile ranges (Fig. 3b-3f) of the pre-event water fraction. It is worth noting that, although the PE1-E1 and PE1-E2 combinations using the TCMM showed the lowest differences, all the $\delta^{18}O$ C_e-C_p combinations showed no statistically significant differences in relation to TrasPAN ($p > 0.05$; Fig. 4).

Similar results were obtained when using EC as tracer for flow partitioning. The combination of PE1 with E1 and E2 also showed the most similar pre-event water fractions as compared to TraSPAN. Differences in maximum, minimum, median and interquartile ranges of the pre-event water fraction were lower than 10 % using these combinations (Fig. 5a). The combination of PE1 with the rest of the C_e values (i.e., E3, E4, E5, and E6) and of PE2 with all C_e values (E1-E6) were higher than 10 % for the minimum pre-event water fractions, but lower than 10 % for the maximum and interquartile ranges of the pre-event water fraction. Differences larger than 10 % for all of the pre-event water fraction pre-event water fraction percentiles were observed for any combination of PE3, PE4, PE5, and PE6 regardless of the C_e value used (Fig. 5c-5f).

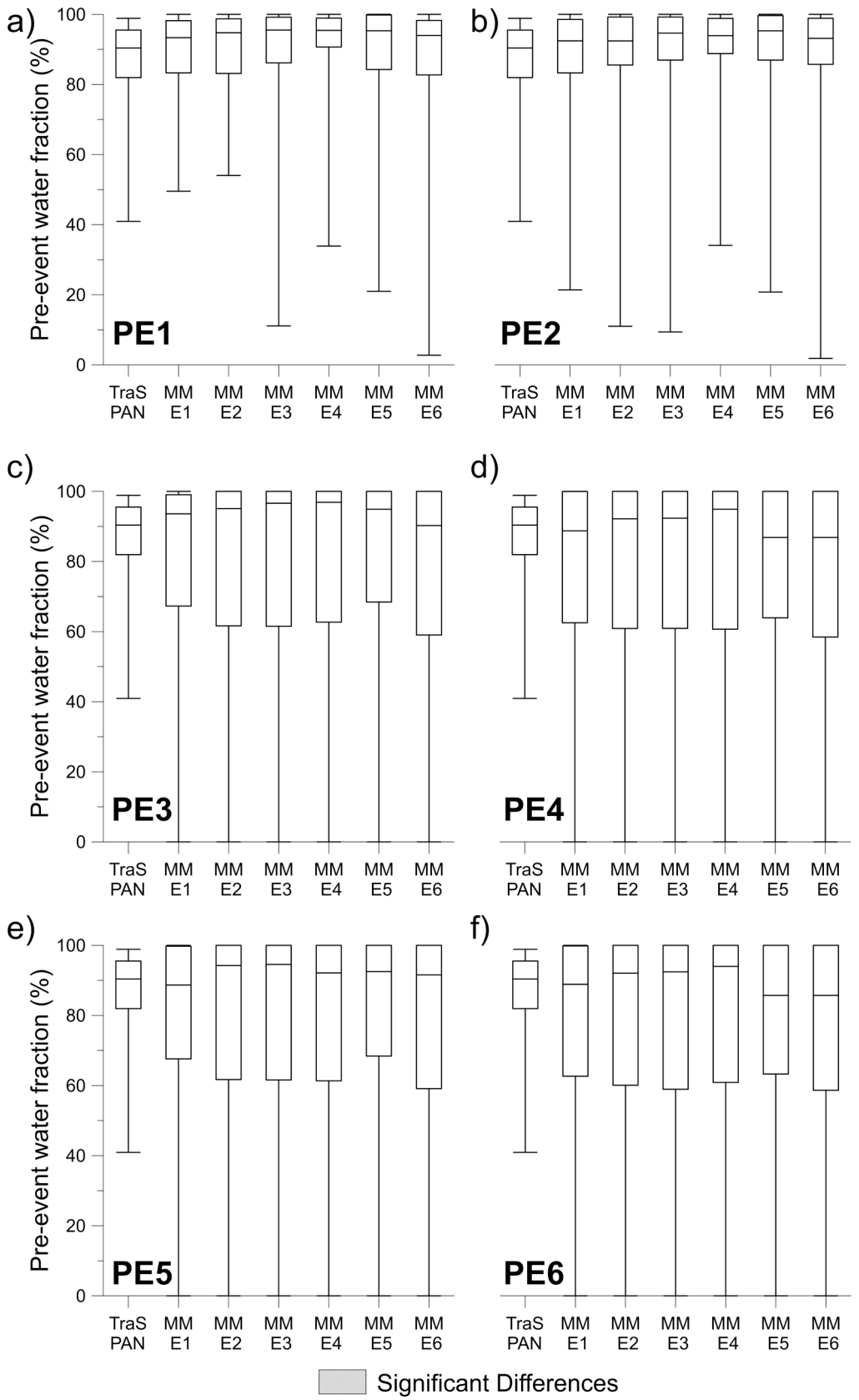

Fig. 3. Pre-event water fractions estimated with TraSPAN and the mixing model (MM) using the isotopic composition of $\delta^{18}O$ as tracer and considering different combinations of event (E1, E2, E3, E4, E5, and E6; see Table 1) and pre-event water samples: a) PE1, b) PE2, c) PE3, d) PE4, e) PE5, and f) PE6 (see Table 1). Filled boxplots indicate statistically significant differences ($p < 0.05$) between the results yielded by TraSPAN and the mixing model with different event and pre-event input data according to the Nemenyi's test.

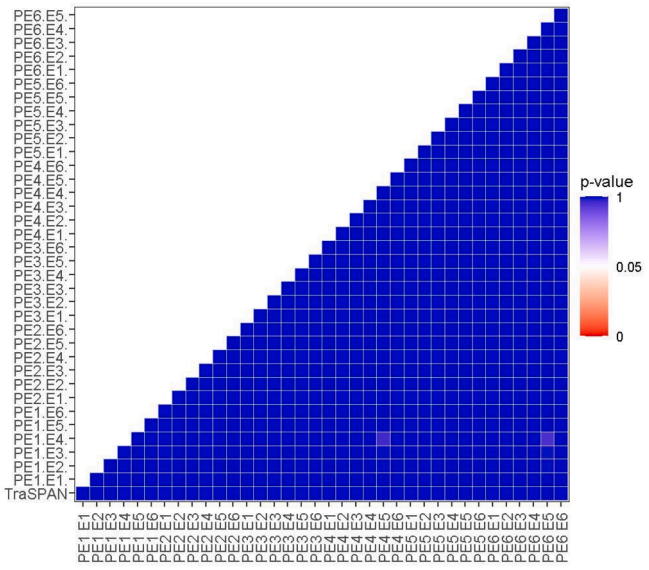

Fig. 4. P-values of the nemenyi's test carried out to compare flow partitioning results yielded by traspan and the mixing model using different combinations of event (e1 to e6) and pre-event water samples (pe1 to pe6) when the isotopic composition of $\delta^{18}O$ is used as tracer. The scale color represents p-values ranging from 0 to 1, where red color means $p = 0$, white $p = 0.05$, and blue $p = 1$, with $p < 0.05$ indicating statistically significant differences. (For interpretation of the references to color in this figure legend, the reader is referred to the web version of this article.)

Statistically significant differences were observed between the TCMM and TraSPAN using EC for all C_e-C_p combinations when using PE5 and PE6 (Fig. 6).

3.5. Comparison of flow partitioning modelling results using ^{18}O and EC

The TraSPAN model yielded similar pre-event water fractions (differences lower than 20 %) for the 37 monitored events regardless of the tracer used for model calibration ($\delta^{18}O$ and EC; Fig. 7). Similar results were observed when using the TCMM for combinations of PE1 with E1 and E2 (Fig. 7a). Differences for PE1 combinations with the other C_e values (i.e., E3 to E6) and the combination of PE2 with all C_e values (E1 to E6) were small (<20 %) for the pre-event water fraction interquartile ranges, but higher than 20 % for the maximum and minimum pre-event water fractions (Fig. 7a-7b). Differences between the results yielded by both tracers were higher for PE3, PE4, PE5, and PE6 regardless of the C_e values used (Fig. 7c-7f). Comparison of the pre-event water fractions using both tracers for all C_e-C_p combinations with PE1, PE2, PE3, and PE4 showed no statistically significant differences ($p > 0.05$; Fig. 8), whereas statistically significant differences were observed when using PE5 and PE6 regardless of the C_e value used. Uncertainty estimations for pre-event water fractions for the 37 rainfall-runoff events ranged from 3 % to 22 % when using $\delta^{18}O$, and from 2 % to 20 % when using EC. Higher values of uncertainty were observed in few events mainly during peak flow (Fig. S2); however; uncertainty generally overlapped during those hydrological conditions.

4. Discussion

4.1. Influence of event and pre-event tracer input data on flow partitioning

The high-resolution tracer monitoring network implemented at the ZEO allowed the evaluation of two flow partitioning models (TraSPAN and TCMM) using $\delta^{18}O$ and EC collected during 37 rainfall-runoff events. The events showed a flashy runoff response to rainfall distinctive of the humid páramo (Mosquera et al., 2015), in which pre-event water fraction dominates streamflow generation (Lazo et al., 2023) via dominant subsurface flow paths (Mosquera et al., 2012; Mosquera et al., 2016a). The weak correlation between the hydrometric characteristics of the events and their peak flow suggests that the latter does not depend on event duration, rainfall amount or intensity.

Regarding the C_e concentration in hydrograph separation research, the average value of rainfall samples has been one of the most common C_e values used in hydrograph separation studies (Klaus and McDonnell, 2013). This, although McDonnell et al. (1990) and Fischer et al. (2017) recommended the use of weighting methods to account for the temporal variation of rainfall amount over the course of a rainstorm. As a result, other studies have considered different C_e alternatives that account for intra-event variation in rainfall amount and tracer signals (e.g., Brown et al., 1999; Kiewiet et al., 2020; Kim et al., 2017; Litt et al., 2015; McGlynn and McDonnell, 2003; Ogunkoya and Jenkins, 1993; Penna et al., 2015). However, comparative analyses of different C_e alternatives are seldom.

Considering the wide range of hydrometeorological conditions across the events monitored at our study site (Table 2), C_e showed no major impact on the estimation of event and pre-event water fractions when using $\delta^{18}O$ or EC (Figs. 3 and 5). Cayuela et al. (2019) also found no significant differences when considering a single sample or a sequential sampling strategy for rainfall concentrations. This effect likely result from the low intra-event variation in the precipitation isotopic composition found during the 37 monitored events. Other studies in Germany and Sweden also reported a small intra-event variability in rainfall isotopic composition (e.g., Orlowski et al., 2016; Rodhe, 1987). The low intra-event variation at the study site could be attributed to a low rainfall amount effect or that there is little to no difference in the source of atmospheric moisture forming local rainfall at event scale (e.g., Crawford et al., 2013; Delavau et al., 2017; Gou et al., 2018; Krklec et al., 2018). This low intra-event variation is key when applying the TCMM, since it complies with model assumption that C_e remains constant over the monitored period (Klaus and McDonnell, 2013); whereas high intra-event variation could increase the uncertainty in hydrograph separation results. Even though the use of bulk rainfall samples could fail to reflect the tracer variability in comparison to higher sampling frequency (Von Freyberg et al., 2017), this is not the case for the ZEO where flow partitioning results were very similar regardless of the event water sample considered.

On the contrary, C_p values showed great influence on the event and pre-event water fractions estimated using $\delta^{18}O$ or EC. When C_p corresponded to stream water samples collected before each of the events (PE1 and PE2, Table S2), the variation of the results was very small. This C_p signal has been frequently used in hydrograph separation studies (e.g., Bonell et al., 1990; McDonnell et al., 1990; Pellerin et al., 2008b; Sklash and Farvolden, 1979; von Freyberg et al., 2018; Von Freyberg et al., 2017) assuming that stream water collected prior to the events is representative of catchment water storage. This finding suggests that the tracers' concentrations of the water stored at the catchment could change from one event to another. This is also in accordance with the Montecarlo approach to estimate C_p in TraSPAN, in which the C_p values that yielded the best results were similar to the PE1 concentrations for all events (Fig. 9). This fingding suggests that for each event specific values of C_p need to be considered for hydrograph separation at our study site, which could result from variable water mixing occurring at the riparian wetlands due to the constant precipitation input (Lazo et al., 2019). Greater differences were identified when C_p was related to the catchment baseflow or low flow averages at yearly to multi-yearly time scales (PE3, PE4, PE5, and PE6) which have been used in other studies (e.g., Bansah and Ali, 2017; Cano-Paoli et al., 2019; Litt et al., 2015; Obradovic and Sklash, 1986; Onda et al., 2006; Pinder and Jones, 1969; Saraiva Okello et al., 2018). This agrees with the study presented by Kiewiet et al. (2020) in a Swiss headwater catchment with a pre- alpine climate, where baseflow did not reflect the catchment average pre-event

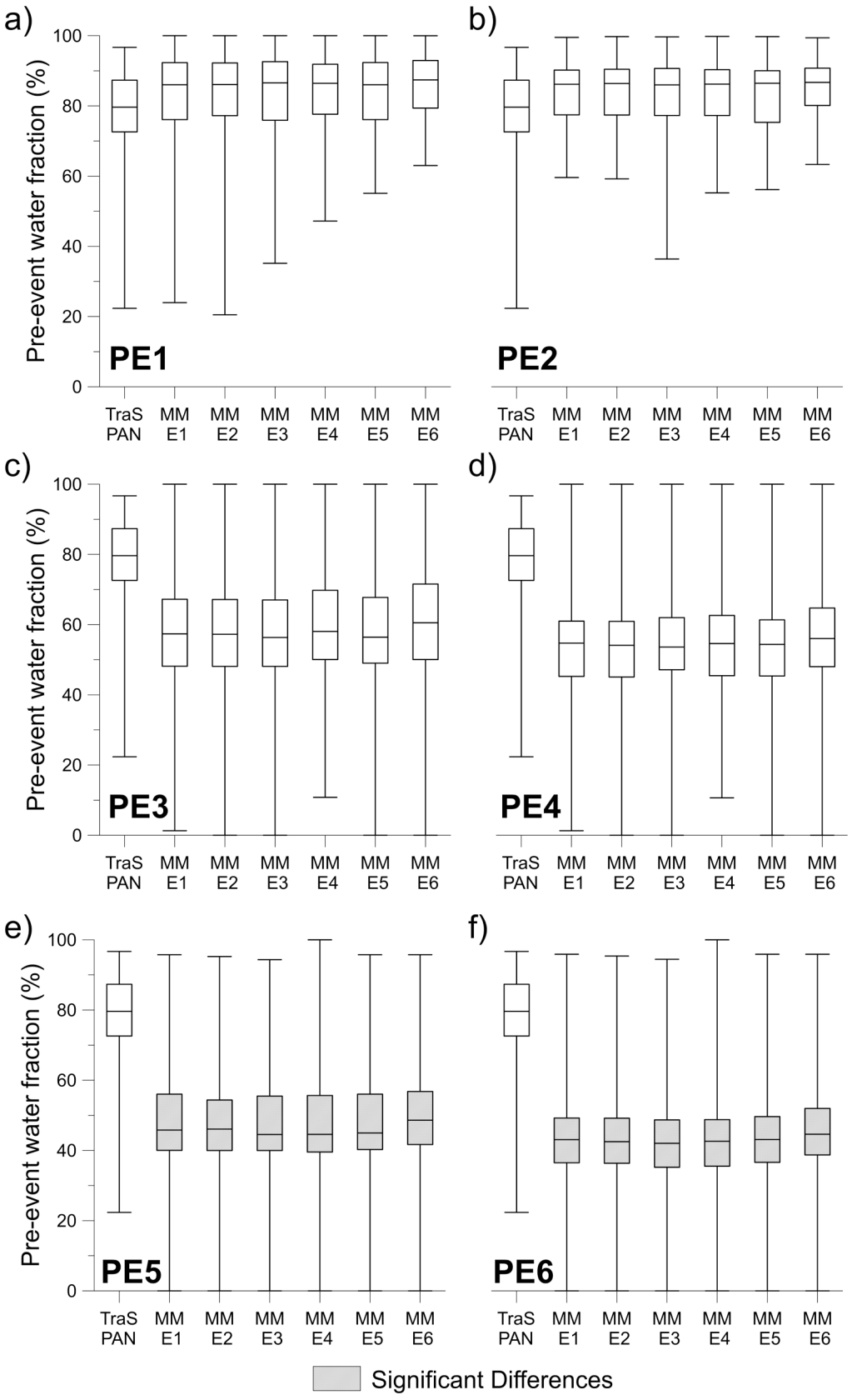

Fig. 5. Pre-event water fractions estimated with TraSPAN and the mixing model (MM) using electrical conductivity as tracer and considering different combinations of event (E1, E2, E3, E4, E5, and E6; see Table 1) and pre-event water samples: a) PE1, b) PE2, c) PE3, d) PE4, e) PE5, and f) PE6. Filled boxplots indicate statistically significant differences ($p < 0.05$) between the results yielded by TraSPAN and the mixing model with different event and pre-event input data according to the Nemenyi's test.

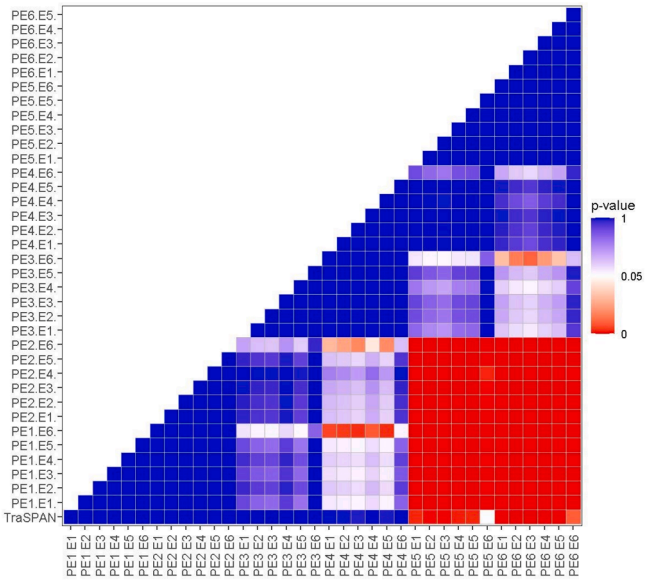

Fig. 6. P-values of the nemenyi's test carried out to compare flow partitioning results yielded by traspan and the mixing model using different combinations of event (e1 to e6) and pre-event water samples (pe1 to pe6) when electrical conductivity is used as tracer. the scale color represents p-values ranging from 0 to 1, in which red color means $p = 0$, white $p = 0.05$, and blue $p = 1$, with $p < 0.05$ indicating statistically significant differences. (For interpretation of the references to color in this figure legend, the reader is referred to the web version of this article.)

concentration adequately. This can be attributed to the fact that not all parts of the catchment are hydrologically connected to the stream during baseflow conditions (e.g., Jencso et al., 2010; Jencso and McGlynn, 2011), and that contributions from different storages change with the expansion of the contributing area and connection of different source areas (Rinderer et al., 2019). These effects have been observed at the ZEO where contributing areas increase as riparian wetlands hydrologically connect to surrounding hillslopes during rainfall events (Correa et al., 2019) depending on antecedent wetness conditions and the amount of precipitation. Similar to our findings, Bansah and Ali (2017) reported that the least accurate C_p definition corresponded to groundwater that is mostly associated with baseflow conditions across 8 nested watersheds in a semiarid Prairie landscape. Therefore, for these systems C_p must be determined for each event based on samples collected prior to the beginning of each event. Future studies in the humid páramo cannot assume that C_p can be represented as constant based on average values from samples collected during baseflow or low flow.

4.2. Comparison of models of different complexity in flow partitioning modelling results

The comparison of the flow partitioning modelling results between the TCMM and the TraSPAN showed very similar event and pre-event water fractions when using PE1 and PE2 regardless of the C_e used for both $\delta^{18}O$ or EC, contrary to the results from PE3, PE4, PE5, and PE6. The similarity of the results between both models, particularly when using PE1, likely results from biophysical conditions of the ZEO in which the presence of riparian wetlands favors the efficient mixing of tracers in the subsurface (Lazo et al., 2023, 2019; Mosquera et al., 2016a). This agrees with the study of Wen et al. (2021) which favors the simple model when comparing two rainfall-runoff models of different complexity (Flux-PIHM and a simple model with two homogeneous well-mixed grids). The authors found that the simple model yielded strong estimations of streamflow under storm conditions in a forested catchment in Pennsylvania (USA). In terms of event and pre-event water fraction estimation during rainfall-runoff events, our findings indicate that models of different complexity could yield similar results when the input tracer concentrations are adequately selected. This clearly shows that the TCMM is still a powerful tool to gain insights into catchment hydrological behavior in the humid páramo despite its simplicity.

4.3. Comparison of flow partitioning modelling results using ^{18}O and EC

EC has been shown to behave as a non-conservative tracer in several hydrograph separation studies (e.g., Blume et al., 2008; Hayashi et al., 2012; Obradovic and Sklash, 1986; Pearce et al., 1986; Penna et al., 2015). This behavior has been attributed to dilution of pre-event water contributions over the course of the events (Litt et al., 2015), to the spatial variability of the contributing water flow paths over time (Hoeg et al., 2000), and/or to differences in the depth of subsurface dominant water flow pathways (Fischer et al., 2017). As a result, the information provided by EC regarding stormflow generation can differ from that yielded by conservative tracers (Klaus and McDonnell, 2013).

Despite the potential constraints of using EC in tracer-aided hydrological studies, other investigations have reported similar flow partitioning modelling results using EC and $\delta^{18}O$ in catchments with different hydrometeorological and biophysical characteristics (e.g., Camacho Suarez et al., 2015; Laudon and Slaymaker, 1997; Meriano et al., 2011; Mosquera et al., 2018). It is however worth highlighting that previous investigation has carried out comparisons between these tracers using datasets with limited representability of hydrological conditions (i.e., a single to a few rainstorm events). The remarkable similarity of event and pre-event water fractions obtained using $\delta^{18}O$ and EC through the simpler TCMM during 37 rainfall-runoff events spanning a wide range of hydrometeorological conditions suggest a quasi-conservative behavior of EC at the study area.

The quasi-conservative behavior of EC at the ZEO likely results from the biophysical characteristics of the catchment. That is, efficient mixing of water in the relatively thin (1–2 m depth) riparian wetland soils (i.e., peat-type Histosols) possessing a high porosity and water holding capacity (Quichimbo et al., 2012), with virtually negligible deep groundwater contributions due to the very low permeability of the underlying bedrock (Pesántez et al., 2023). As a result, the riparian wetland soils represent the main water storage (Lazo et al., 2019) and source of water contributing to streamflow generation year-round (Correa et al., 2017; Mosquera et al., 2016a). The soil hydrological behavior in combination with sustained inputs of low intensity precipitation in turn is likely to diminish the spatial and temporal variation of EC due to internal catchment hydrochemical processes, explaining the quasi-conservative behavior of this tracer at the ZEO (Mosquera et al., 2016b).

Methodologically, this effect contributes the hydrological system to accomplish one of the key TCMM assumptions regarding the contribution of the pre-event (or subsurface) water end-member to flow partitioning: "Contributions from the vadose zone must be negligible, or the isotopic signature of the soil water must be similar to that of groundwater."(Klaus and McDonnell, 2013). At the ZEO, the pre-event water component is almost exclusively composed of subsurface water stored in the well-mixed riparian wetland soil water reservoir, which represents 80–100 % of total flow during the monitored events (Figs. 3 and 5). In addition, the similarity in pre-event water fractions was generally observed throughout the whole duration of the rainfall-runoff events (i.e., rising limb, peak, and falling limb; Fig S2.) with some exceptions at peak flow. These findings partially agree with those reported by Wang et al. (2019) who determined that the best time to collect stream water samples for tracer-aided hydrograph separation analysis was before the storm and at the recession limb. Complementarily, the use of EC yielded a reduced uncertainty for determining event and pre-event water fractions due to the smaller relative uncertainty in the analytical measurement of this tracer compared to $\delta^{18}O$ should a correct selection of the C_e and C_p source concentrations was achieved as demonstrated in our analyses, where higher uncertainties are observed mostly at peak flows.

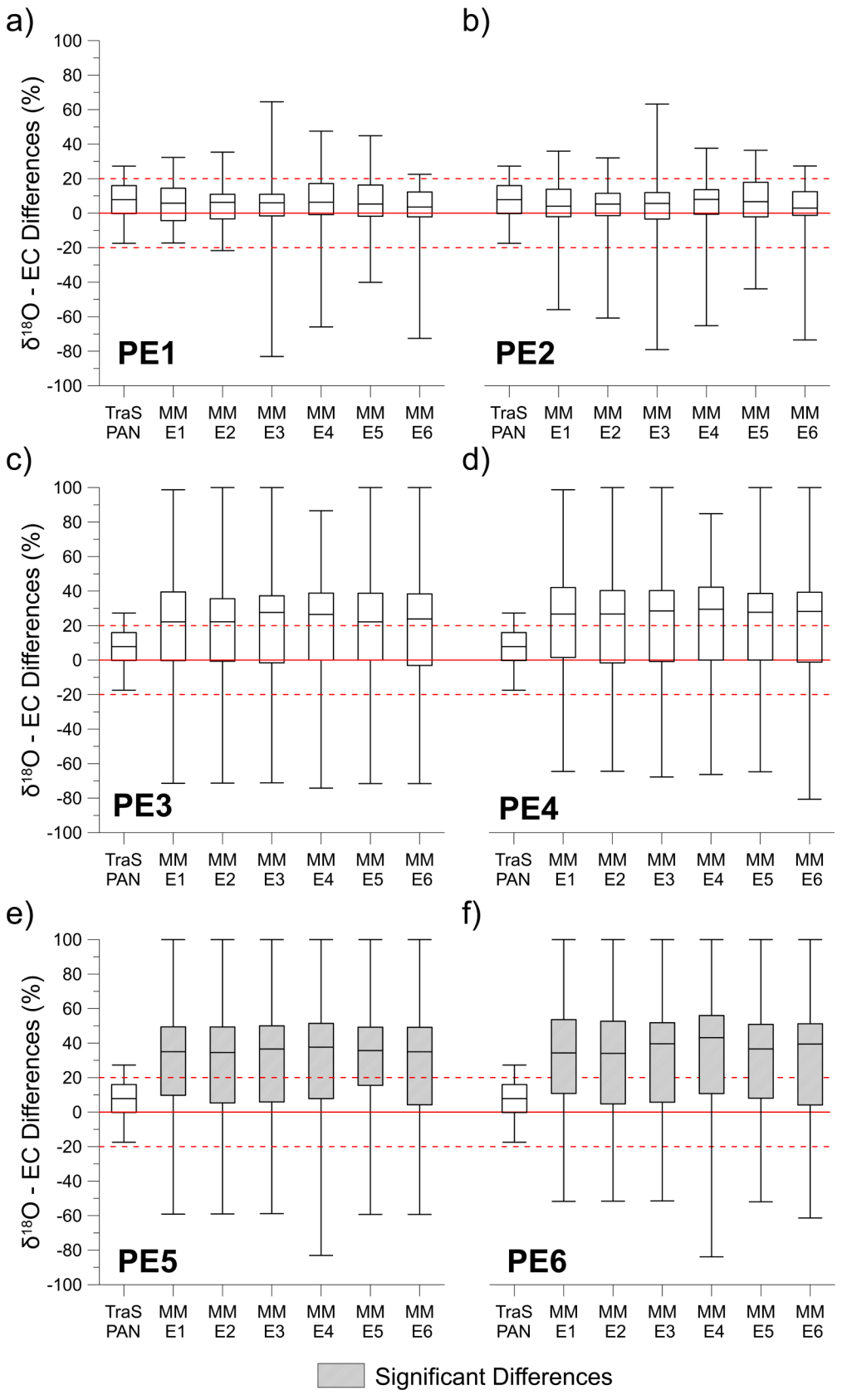

Fig. 7. Differences in pre-event water fractions estimated using different tracer (i.e., the isotopic composition, $\delta^{18}O$ and electrical conductivity, EC) with TraSPAN and the mixing model (MM) and considering different combinations of event (E1, E2, E3, E4, E5, and E6) and pre-event water samples: a) PE1, b) PE2, c) PE3, d) PE4, e) PE5, and f) PE6. Filled boxplots indicate statistically significant differences ($p < 0.05$) between the results yielded by $\delta^{18}O$ and EC according to the Nemenyi's test.

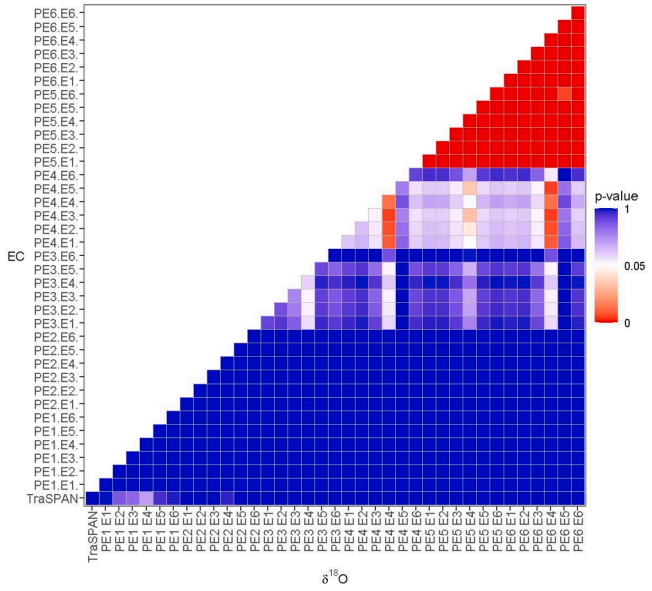

Fig. 8. P-values of the nemenyi's test carried out to compare flow partitioning results yielded by the isotopic composition of $\delta^{18}O$ and electrical conductivity (EC) using TraSPAN and the mixing model with different combinations of event (E1 to E6) and pre-event water samples (PE1 to PE6). The scale color represents p-values ranging from 0 to 1, in which red color means $p = 0$, white $p = 0.05$, and blue $p = 1$, with $p < 0.05$ indicating statistically significant differences. (For interpretation of the references to color in this figure legend, the reader is referred to the web version of this article.)

These could be attributed to the fact that at peak flows systems often have a non-linear behavior which could amplify the uncertainties.

Overall, our findings encourage the use of EC as a surrogate of $\delta^{18}O$ to estimate the event and pre-event components of streamflow at the ZEO to take advantage of its benefits including ease of measurement at high temporal frequency and low operational and maintenance monitoring cost (Cano-Paoli et al., 2019). These findings agree with past investigations in which similar results have been obtained in catchments with certain biophysical characteristics in which EC has been shown to behave conservatively (Bansah et al., 2019). Regionally, it has been demonstrated that the hydrological behavior of the ZEO is representative of páramo catchments in south Ecuador in which topographical, vegetation, soil, and geological conditions are similar (Mosquera et al., 2023; Ramón et al., 2021). We also expect that based on our findings the use of EC in hydrograph separation studies could be further extended to regions with biophysical conditions similar to those of the high-Andean páramo, i.e., where hydrological behavior is dominated by peat-type riparian soils with little to no contributions of deep groundwater flow to total streamflow (e.g., the Scottish highlands; Geris et al., 2017, 2015; Tetzlaff et al., 2014).

Nevertheless, our work highlights that the appropriate characterization of C_p is crucial to obtain reliable flow partitioning results using EC in such environments. The continuous monitoring of EC at high temporal frequency and at low cost will increase the availability of data to adequately assess C_p, replacing the isotopic high-resolution monitoring that is uncommon to achieve and maintain over long periods of time. These benefits in turn, can allow the use of tracer-aided hydrological information for water management and the identification of long-term changes in hydrological conditions as a result of changes in land use and climate as they permit the continuous monitoring of stream water tracer data at high temporal frequency.

5. Conclusions

This study highlights the need to appropriately assess the selection of event and pre-event water samples in hydrograph separation analyses using stable isotopes ($\delta^{18}O$) and electrical conductivity (EC). Our findings for 37 rainfall-runoff events presenting different hydrometeorological conditions in the humid Andes páramo shows that the selection of event and pre-event water samples must be specific for each event analyzed regarding of the tracer used. The tracer signal of a stream water sample collected prior to the beginning of each event was identified as the most representative of the pre-event water signal. This finding clearly suggests that the use of a single value (e.g., the average of baseflow or low flow during yearly of semi-yearly periods) for all the events should be avoided to obtain reliable hydrograph separation results in the study region. We also found that the temporal variability of event water tracer signals has little to no influence on flow partitioning results mainly because of the small intra-event variation of the rainfall tracer concentration. Our findings indicate that a single sample collected during each event is sufficient to provide robust hydrograph separation results regardless of the tracer used. Overall, these findings remark the importance of focusing high-resolution sampling efforts to stream water for determining the pre-event water concentration for hydrograph separation.

The comparison of hydrograph separation models of different complexity, namely a two-component mixing model (TCMM; low mathematical complexity) and a tracer-aided hydrological model (TAHM; high mathematical and computational complexity), showed that both models estimate similar event and pre-event water fractions for all events regardless of the tracer used. Thus, the use of a simple mixing model in the humid páramo improves the understanding of rainfall-runoff catchment response while reducing the computational time and resources allocated in modeling. In addition, the fact that EC yields similar results than $\delta^{18}O$ using both models facilitate the collection of stream water samples at high temporal frequency (sub-hourly) to be used in hydrograph separation studies in the humid páramo in order to appropriately select the pre-event water signal. The combination of a simple mathematical framework (TCMM) and high-resolution tracer sampling (EC) not only allows to lower the logistical and economical resources needed to adequately assess hydrograph separation, but also sheds light on a unique opportunity to carry out quasi-continuous assessments of flow partitioning with high accuracy in high-Andean catchments that generally remain poorly gauged to ungauged in the region. This opportunity is highly valuable to progress the understanding of catchment hydrology in the region to support water management of humid páramo catchments.

Funding

This research was funded by the DFG RESPECT 386807763 and the Vice-rectorate of Investigation of the University of Cuenca (VIUC) through the project "From field scale eco-hydrological process understanding to landscape scale water fluxes". CS was supported by the National Science Foundation Award No. 1943574.

CRediT authorship contribution statement

Patricio X. Lazo: Writing – review & editing, Writing – original draft, Software, Methodology, Investigation, Formal analysis, Data curation, Conceptualization. **Giovanny M. Mosquera:** Writing – review & editing, Validation, Supervision, Resources, Investigation, Conceptualization. **Irene Cárdenas:** Resources, Methodology, Formal analysis. **Catalina Segura:** Writing – review & editing, Validation, Supervision, Software, Investigation, Funding acquisition, Formal analysis. **Patricio Crespo:** Writing – review & editing, Validation, Supervision, Resources, Project administration, Investigation, Funding acquisition, Formal analysis, Conceptualization.

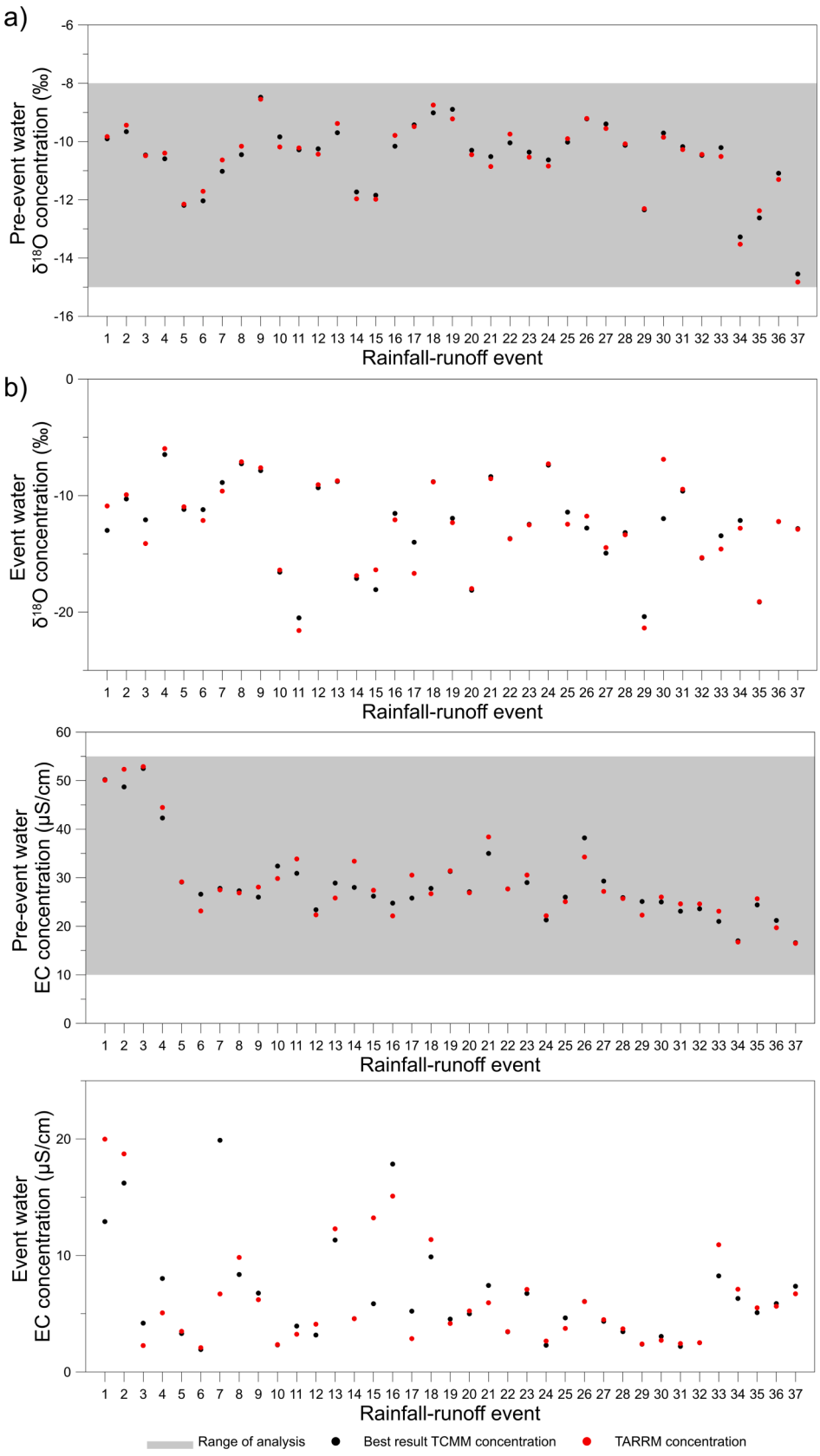

Fig. 9. Comparison of the $\delta^{18}O$ (a and b) and electrical conductivity (EC; c and d) pre-event and event water samples used for flow partitioning with TraSPAN (red dots) and the mixing model that yielded the best results (i.e., using PE1 as pre-event water sample) for all monitored events. Note the wide range of pre-event tracer concentrations observed during the monitored events (gray shaded area in a and c). (For interpretation of the references to color in this figure legend, the reader is referred to the web version of this article.)

Declaration of competing interest

The authors declare that they have no known competing financial interests or personal relationships that could have appeared to influence the work reported in this paper.

Data availability

Data will be made available on request.

Acknowledgments

This manuscript is an outcome of the University of Cuenca's Doctoral Program in Water Resources. The authors would like to thank Dundee Precious Metals Ecuador S.A. staff for their assistance in the logistics at the Zhurucay Ecohydrological Observatory. We also thank Franklin Marín, Juan Pesántez, Mishelle Palacios, Viviana Arízaga, Pablo Peña, Juan Cabrera, and Karina Larco for their support with the collection of water samples and hydrometeorological data.

Appendix A. Supplementary data

Supplementary data to this article can be found online at https://doi.org/10.1016/j.jhydrol.2024.131632.

References

Bansah, S., Ali, G., 2017. Evaluating the effects of tracer choice and end-member definitions on hydrograph separation results across nested, seasonally cold watersheds. Water Resour. Res. 53, 8851–8871. https://doi.org/10.1002/2016WR020252.

Bansah, S., Quaye-ballard, J., Andam-akorfu, S.A., Bam, E., Anornu, G.K., 2019. End-member selection in two-component isotope-based hydrograph separation. Open J. Mod. Hydrol. 9, 41–53. https://doi.org/10.4236/ojmh.2019.92003.

Beven, K., Binley, A., 1992. The future of distributed models: Model calibration and uncertainty prediction. Hydrol. Process. 6, 279–298. https://doi.org/10.1002/hyp.3360060305.

Beven, K., Freer, J., 2001. Equifinality, data assimilation, and uncertainty estimation in mechanistic modelling of complex environmental systems using the GLUE methodology. J. Hydrol. 249, 11–29. https://doi.org/10.1016/S0022-1694(01)00421-8.

Birkel, C., Dunn, S.M., Tetzlaff, D., Soulsby, C., 2010. Assessing the value of high-resolution isotope tracer data in the stepwise development of a lumped conceptual rainfall–runoff model. Hydrol. Process. 24, 2335–2348. https://doi.org/10.1002/HYP.7763.

Birkel, C., Soulsby, C., 2015. Advancing tracer-aided rainfall-runoff modelling: a review of progress, problems and unrealised potential. Hydrol. Process. 29, 5227–5240. https://doi.org/10.1002/hyp.10594.

Birkel, C., Soulsby, C., Tetzlaff, D., 2014. Developing a consistent process-based conceptualization of catchment functioning using measurements of internal state variables. Water Resour. Res. 50, 3481–3501. https://doi.org/10.1002/2013WR014925.

Blume, T., Zehe, E., Bronstert, A., 2008. Investigation of runoff generation in a pristine, poorly gauged catchment in the Chilean Andes II: Qualitative and quantitative use of tracers at three spatial scales. Hydrol. Process. 22, 3676–3688. https://doi.org/10.1002/HYP.6970.

Bonell, M., Pearce, A.J., Stewart, M.K., 1990. The identification of runoff-production mechanisms using environmental isotopes in a tussock grassland catchment, eastern otago, New Zealand. Hydrol. Process. 4, 15–34. https://doi.org/10.1002/HYP.3360040103.

Brown, V.A., McDonnell, J.J., Burns, D.A., Kendall, C., 1999. The role of event water, a rapid shallow flow component, and catchment size in summer stormflow. J. Hydrol. 217, 171–190. https://doi.org/10.1016/S0022-1694(98)00247-9.

Camacho Suarez, V.V., Saraiva Okello, A.M.L., Wenninger, J.W., Uhlenbrook, S., Suarez, C., 2015. Understanding runoff processes in a semi-arid environment through isotope and hydrochemical hydrograph separations. Hydrol. Earth Syst. Sci 19, 4183–4199. https://doi.org/10.5194/hess-19-4183-2015.

Cano-Paoli, K., Chiogna, G., Bellin, A., 2019. Convenient use of electrical conductivity measurements to investigate hydrological processes in Alpine headwaters. Sci. Total Environ. 685, 37–49. https://doi.org/10.1016/J.SCITOTENV.2019.05.166.

Cartwright, I., Morgenstern, U., 2018. Using tritium and other geochemical tracers to address the "old water paradox" in headwater catchments. J. Hydrol. 563, 13–21. https://doi.org/10.1016/j.jhydrol.2018.05.060.

Cayuela, C., Latron, J., Geris, J., Llorens, P., 2019. Spatio-temporal variability of the isotopic input signal in a partly forested catchment: Implications for hydrograph separation. Hydrol. Process. 33, 36–46. https://doi.org/10.1002/hyp.13309.

Cey, E.E., Rudolph, D.L., Parkin, G.W., Aravena, R., 1998. Quantifying groundwater discharge to a small perennial stream in southern Ontario. Canada. J. Hydrol. 210, 21–37. https://doi.org/10.1016/S0022-1694(98)00172-3.

Correa, A., Windhorst, D., Tetzlaff, D., Crespo, P., Célleri, R., Feyen, J., Breuer, L., 2017. Temporal dynamics in dominant runoff sources and flow paths in the Andean Páramo. Water Resour. Res. 53, 5998–6017. https://doi.org/10.1002/2016WR020187.

Correa, A., Breuer, L., Crespo, P., Célleri, R., Feyen, J., Birkel, C., Silva, C., Windhorst, D., 2019. Spatially distributed hydro-chemical data with temporally high-resolution is needed to adequately assess the hydrological functioning of headwater catchments. Sci. Total Environ. 651, 1613–1626. https://doi.org/10.1016/J.SCITOTENV.2018.09.189.

Crawford, J., Hughes, C.E., Parkes, S.D., 2013. Is the isotopic composition of event based precipitation driven by moisture source or synoptic scale weather in the Sydney Basin, Australia? J. Hydrol. 507, 213–226. https://doi.org/10.1016/J.JHYDROL.2013.10.031.

Delavau, C.J., Stadnyk, T., Holmes, T., 2017. Examining the impacts of precipitation isotope input δ18O ppt) on distributed, tracer-aided hydrological modelling. Hydrol. Earth Syst. Sci. 21, 2595–2614. https://doi.org/10.5194/HESS-21-2595-2017.

Detty, J.M., McGuire, K.J., 2010. Threshold changes in storm runoff generation at a till-mantled headwater catchment. Water Resour. Res. 46 https://doi.org/10.1029/2009WR008102.

Dunkerley, D., 2008. Identifying individual rain events from pluviograph records: a review with analysis of data from an Australian dryland site. Hydrol. Process. 22, 5024–5036. https://doi.org/10.1002/hyp.7122.

Dunn, S.M., Freer, J., Weiler, M., Kirkby, M.J., Seibert, J., Quinn, P.F., Lischeid, G., Tetzlaff, D., Soulsby, C., 2008. Conceptualization in catchment modelling: simply learning? Hydrol. Process. 22, 2389–2393. https://doi.org/10.1002/hyp.7070.

Durand, P., Neal, M., Neal, C., 1993. Variations in stable oxygen isotope and solute concentrations in small submediterranean montane streams. J. Hydrol. 144, 283–290. https://doi.org/10.1016/0022-1694(93)90176-A.

Esquivel-Hernández, G., Mosquera, G.M., Sánchez-Murillo, R., Quesada-Román, A., Birkel, C., Crespo, P., Célleri, R., Windhorst, D., Breuer, L., Boll, J., 2019. Moisture transport and seasonal variations in the stable isotopic composition of rainfall in Central American and Andean Páramo during El Niño conditions (2015–2016). Hydrol. Process. 33, 1802–1817. https://doi.org/10.1002/hyp.13438.

Fenicia, F., McDonnell, J.J., Savenije, H.H.G., 2008. Learning from model improvement: On the contribution of complementary data to process understanding. Water Resour. Res. 44 https://doi.org/10.1029/2007WR006386.

Fischer, B.M.C., van Meerveld (Ilja), H.J., Seibert, J., 2017. Spatial variability in the isotopic composition of rainfall in a small headwater catchment and its effect on hydrograph separation. J. Hydrol. 547, 755–769. https://doi.org/10.1016/j.jhydrol.2017.01.045.

Floury, P., Gaillardet, J., Gayer, E., Bouchez, J., Tallec, G., Ansart, P., Koch, F., Gorge, C., Blanchouin, A., Roubaty, J.L., 2017. The potamochemical symphony: New progress in the high-frequency acquisition of stream chemical data. Hydrol. Earth Syst. Sci. 21, 6153–6165. https://doi.org/10.5194/HESS-21-6153-2017.

Genereux, D., 1998. Quantifying uncertainty in tracer-based hydrograph separations. Water Resour. Res. 34, 915–919. https://doi.org/10.1029/98WR00010.

Geris, J., Tetzlaff, D., Soulsby, C., 2015. Resistance and resilience to droughts: hydropedological controls on catchment storage and run-off response. Hydrol. Process. 29, 4579–4593. https://doi.org/10.1002/hyp.10480.

Geris, J., Tetzlaff, D., McDonnell, J.J., Soulsby, C., 2017. Spatial and temporal patterns of soil water storage and vegetation water use in humid northern catchments. Sci. Total Environ. 595, 486–493. https://doi.org/10.1016/j.scitotenv.2017.03.275.

Goller, R., Wilcke, W., Leng, M.J., Tobschall, H.J., Wagner, K., Valarezo, C., Zech, W., 2005. Tracing water paths through small catchments under a tropical montane rain forest in south Ecuador by an oxygen isotope approach. J. Hydrol. 308, 67–80. https://doi.org/10.1016/j.jhydrol.2004.10.022.

Gou, J., Qu, S., Shi, P., Li, D., Chen, X., Wang, Y., Shan, S., Si, W., 2018. Application of Stable Isotope Tracer to Study Runoff Generation during Different Types of Rainfall Events. Water 2018, Vol. 10, Page 538 10, 538. 10.3390/W10050538.

Guallpa, M., Célleri, R., Crespo, P., 2022. Efecto del coeficiente teórico de descarga de vertederos sobre la medición de caudales en pequeños ríos Andinos. La Granja 36. https://doi.org/10.17163/LGR.N36.2022.06.

Gupta, H.V., Kling, H., Yilmaz, K.K., Martinez, G.F., 2009. Decomposition of the mean squared error and NSE performance criteria: Implications for improving hydrological modelling. J. Hydrol. 377, 80–91. https://doi.org/10.1016/j.jhydrol.2009.08.003.

Harman, C.J., 2015. Time-variable transit time distributions and transport: Theory and application to storage-dependent transport of chloride in a watershed. Water Resour. Res. 51, 1–30. https://doi.org/10.1002/2014WR015707.

Hayashi, M., Vogt, T., Mächler, L., Schirmer, M., 2012. Diurnal fluctuations of electrical conductivity in a pre-alpine river: Effects of photosynthesis and groundwater exchange. J. Hydrol. 450–451, 93–104. https://doi.org/10.1016/J.JHYDROL.2012.05.020.

Hoeg, S., Uhlenbrook, S., Leibundgut, C., 2000. Hydrograph separation in a mountainous catchment ? combining hydrochemical and isotopic tracers. Hydrol. Process. 14, 1199–1216. https://doi.org/10.1002/(SICI)1099-1085(200005)14:7<1199::AID-HYP35>3.0.CO;2-K.

Hollander, M., Wolfe, D.A., Chicken, E., 2013. Nonparametric statistical methods. Wiley Series in Probability and Statistics. Wiley.

Hooper, R.P., Shoemaker, C.A., 1986. A Comparison of Chemical and Isotopic Hydrograph Separation. Water Resour. Res. 22, 1444–1454. https://doi.org/10.1029/WR022i010p01444.

IUSS Working Group WRB, 2015. World Reference Base for Soil Resources 2014, update 2015. International soil classification system for naming soils and creating legends for soil maps. World Soil Resources Reports No. 106. FAO Rome.
Iwagami, S., Tsujimura, M., Onda, Y., Shimada, J., Tanaka, T., 2010. Role of bedrock groundwater in the rainfall-runoff process in a small headwater catchment underlain by volcanic rock. Hydrol. Process. 24, 2771–2783. https://doi.org/10.1002/hyp.7690.
Jakeman, A.J., Hornberger, G.M., 1993. How much complexity is warranted in a rainfall-runoff model? Water Resour. Res. 29, 2637–2649. https://doi.org/10.1029/93WR00877.
Jencso, K.G., McGlynn, B.L., 2011. Hierarchical controls on runoff generation: Topographically driven hydrologic connectivity, geology, and vegetation. Water Resour. Res. 47, 11527. https://doi.org/10.1029/2011WR010666.
Jencso, K.G., McGlynn, B.L., Gooseff, M.N., Bencala, K.E., Wondzell, S.M., 2010. Hillslope hydrologic connectivity controls riparian groundwater turnover: Implications of catchment structure for riparian buffering and stream water sources. Water Resour. Res. 46, 10524. https://doi.org/10.1029/2009WR008818.
Johnson, K., Harpold, A., Carroll, R.W.H., Barnard, H., Raleigh, M.S., Segura, C., Li, L., Williams, K.H., Dong, W., Sullivan, P.L., 2023. Leveraging Groundwater Dynamics to Improve Predictions of Summer Low-Flow Discharges. Water Resour. Res. 59 https://doi.org/10.1029/2023WR035126.
Kendall, C., McDonnell, J.J., 1998. Isotope tracers in catchment hydrology. Elsevier.
Kiewiet, L., van Meerveld, I., Seibert, J., 2020. Effects of Spatial Variability in the Groundwater Isotopic Composition on Hydrograph Separation Results for a Pre-Alpine Headwater Catchment. Water Resour. e2019WR026855 Res. 56. https://doi.org/10.1029/2019WR026855.
Kim, H., Cho, S.-H., Lee, D., Jung, Y.-Y., Kim, Y.-H., Koh, D.-C., Lee, J., 2017. Influence of pre-event water on streamflow in a granitic watershed using hydrograph separation. Environ. Earth Sci. 76, 82. https://doi.org/10.1007/s12665-017-6402-6.
Klaus, J., McDonnell, J.J., 2013. Hydrograph separation using stable isotopes: Review and evaluation. J. Hydrol. 505, 47–64. https://doi.org/10.1016/j.jhydrol.2013.09.006.
Krklec, K., Domínguez-Villar, D., Lojen, S., 2018. The impact of moisture sources on the oxygen isotope composition of precipitation at a continental site in central Europe. J. Hydrol. 561, 810–821. https://doi.org/10.1016/J.JHYDROL.2018.04.045.
Lang, M., Ouarda, T.B.M.J., Bobée, B., 1999. Towards operational guidelines for over-threshold modeling. J. Hydrol. https://doi.org/10.1016/S0022-1694(99)00167-5.
Larco, K., Mosquera, G.M., Jacobs, S.R., Cardenas, I., Crespo, P., 2023. Factors controlling the temporal variability of streamflow transit times in tropical alpine catchments. J. Hydrol. 617, 128990 https://doi.org/10.1016/J.JHYDROL.2022.128990.
Laudon, H., Slaymaker, O., 1997. Hydrograph separation using stable isotopes, silica and electrical conductivity: an alpine example. J. Hydrol. 201, 82–101. https://doi.org/10.1016/S0022-1694(97)00030-9.
Lazo, P.X., Mosquera, G.M., McDonnell, J.J., Crespo, P., 2019. The role of vegetation, soils, and precipitation on water storage and hydrological services in Andean Páramo catchments. J. Hydrol. 572, 805–819. https://doi.org/10.1016/J.JHYDROL.2019.03.050.
Lazo, P.X., Mosquera, G.M., Cárdenas, I., Segura, C., Crespo, P., 2023. Flow partitioning modelling using high-resolution electrical conductivity data during variable flow conditions in a tropical montane catchment. J. Hydrol. 617, 128898 https://doi.org/10.1016/J.JHYDROL.2022.128898.
Leaney, F.W., Smettem, K.R.J., Chittleborough, D.J., 1993. Estimating the contribution of preferential flow to subsurface runoff from a hillslope using deuterium and chloride. J. Hydrol. 147, 83–103. https://doi.org/10.1016/0022-1694(93)90076-L.
Lee, J.-Y., Shih, Y.-T., Lan, C.-Y., Lee, T.-Y., Peng, T.-R., Lee, C.-T., Huang, J.-C., 2020. Rainstorm Magnitude Likely Regulates Event Water Fraction and Its Transit Time in Mesoscale Mountainous Catchments: Implication for Modelling Parameterization. Water 12, 1169. https://doi.org/10.3390/w12041169.
Litt, G.F., Gardner, C.B., Ogden, F.L., Lyons, W.B., 2015. Hydrologic tracers and thresholds: A comparison of geochemical techniques for event-based stream hydrograph separation and flowpath interpretation across multiple land covers in the Panama Canal Watershed. Appl. Geochemistry 63, 507–518. https://doi.org/10.1016/J.APGEOCHEM.2015.04.003.
Liu, F., Williams, M.W., Caine, N., 2004. Source waters and flow paths in an alpine catchment, Colorado Front Range. United States. Water Resour. Res. 40 https://doi.org/10.1029/2004WR003076.
Lyon, S.W., Desilets, S.L.E., Troch, P.A., 2008. Characterizing the response of a catchment to an extreme rainfall event using hydrometric and isotopic data. Water Resour. Res. 44 https://doi.org/10.1029/2007WR006259.
McDonnell, J.J., Bonell, M., Stewart, M.K., Pearce, A.J., 1990. Deuterium variations in storm rainfall: Implications for stream hydrograph separation. Water Resour. Res. 26, 455–458. https://doi.org/10.1029/WR026I003P00455.
McGlynn, B.L., McDonnell, J.J., 2003. Quantifying the relative contributions of riparian and hillslope zones to catchment runoff. Water Resour. Res. 39, 1310–1330. https://doi.org/10.1029/2003WR002091.
McGlynn, B.L., McDonnell, J.J., Seibert, J., Kendall, C., 2004. Scale effects on headwater catchment runoff timing, flow sources, and groundwater-streamflow relations. Water Resour. Res. 40 https://doi.org/10.1029/2003WR002494.
McGuire, K.J., McDonnell, J.J., 2006. A review and evaluation of catchment transit time modeling. J. Hydrol. 330, 543–563. https://doi.org/10.1016/j.jhydrol.2006.04.020.
Meriano, M., Howard, K.W.F., Eyles, N., 2011. The role of midsummer urban aquifer recharge in stormflow generation using isotopic and chemical hydrograph separation techniques. J. Hydrol. 396, 82–93. https://doi.org/10.1016/J.JHYDROL.2010.10.041.
Monteith, S.S., Buttle, J.M., Hazlett, P.W., Beall, F.D., Semkin, R.G., Jeffries, D.S., 2006. Paired-basin comparison of hydrologic response in harvested and undisturbed hardwood forests during snowmelt in central Ontario: II. Streamflow sources and groundwater residence times. Hydrol. Process. 20, 1117–1136. https://doi.org/10.1002/hyp.6073.
Mosquera, G.M., Célleri, R., Lazo, P.X., Vaché, K.B., Perakis, S.S., Crespo, P., 2016a. Combined use of isotopic and hydrometric data to conceptualize ecohydrological processes in a high-elevation tropical ecosystem. Hydrol. Process. 30, 2930–2947. https://doi.org/10.1002/hyp.10927.
Mosquera, G.M., Franklin, M., Jan, F., Rolando, C., Lutz, B., David, W., Patricio, C., 2021. A field, laboratory, and literature review evaluation of the water retention curve of volcanic ash soils: How well do standard laboratory methods reflect field conditions? Hydrol. Process. 35 https://doi.org/10.1002/hyp.14011.
Mosquera, G.M., Hofstede, R., Bremer, L.L., Asbjornsen, H., Carabajo-Hidalgo, A., Célleri, R., Crespo, P., Esquivel-Hernández, G., Feyen, J., Manosalvas, R., Marín, F., Mena-Vásconez, P., Montenegro-Díaz, P., Ochoa-Sánchez, A., Pesántez, J., Riveros-Iregui, D.A., Suárez, E., 2023. Frontiers in páramo water resources research: A multidisciplinary assessment. Sci. Total Environ. 892, 164373 https://doi.org/10.1016/j.scitotenv.2023.164373.
Mosquera, G., Lazo, P., Cárdenas, I., Crespo, P., 2012. Identificación de las principales fuentes de agua que aportan a la generación de escorrentía en zonas Andinas de páramo húmedo: mediante el uso de los isótopos estables deuterio (δ 2 H) y oxígeno-18 (δ 18 O). Maskana 3, 87–105.
Mosquera, G.M., Lazo, P.X., Célleri, R., Wilcox, B.P., Crespo, P., 2015. Runoff from tropical alpine grasslands increases with areal extent of wetlands. Catena 125, 120–128. https://doi.org/10.1016/j.catena.2014.10.010.
Mosquera, G.M., Segura, C., Vaché, K.B., Windhorst, D., Breuer, L., Crespo, P., 2016b. Insights into the water mean transit time in a high-elevation tropical ecosystem. Hydrol. Earth Syst. Sci. 20, 2987–3004. https://doi.org/10.5194/hess-20-2987-2016.
Mosquera, G., Segura, C., Crespo, P., Mosquera, G.M., Segura, C., Crespo, P., 2018. Flow Partitioning Modelling Using High-Resolution Isotopic and Electrical Conductivity Data. Water 10, 904. https://doi.org/10.3390/w10070904.
Muñoz-Villers, L.E., McDonnell, J.J., 2012. Runoff generation in a steep, tropical montane cloud forest catchment on permeable volcanic substrate. Water Resour. Res. 48, n/a-n/a. https://doi.org/10.1029/2011WR011316.
Munyaneza, O., Wenninger, J., Uhlenbrook, S., 2012. Identification of runoff generation processes using hydrometric and tracer methods in a meso-scale catchment in Rwanda. Hydrol. Earth Syst. Sci. 16, 1991–2004. https://doi.org/10.5194/hess-16-1991-2012.
Nolan, K.M., Hill, B.R., 1990. Storm-runoff generation in the Permanente Creek drainage basin, west central California — An example of flood-wave effects on runoff composition. J. Hydrol. 113, 343–367. https://doi.org/10.1016/0022-1694(90)90183-X.
Obradovic, M.M., Sklash, M.G., 1986. An isotopic and geochemical study of snowmelt runoff in a small arctic watershed. Hydrol. Process. 1, 15–30. https://doi.org/10.1002/HYP.3360010104.
Ochoa-Sánchez, A.E., Crespo, P., Carrillo-Rojas, G., Marín, F., Célleri, R., 2020. Unravelling evapotranspiration controls and components in tropical Andean tussock grasslands. Hydrol. Process. 34, 2117–2127. https://doi.org/10.1002/HYP.13716.
Ogunkoya, O.O., Jenkins, A., 1993. Analysis of storm hydrograph and flow pathways using a three-component hydrograph separation model. J. Hydrol. 142, 71–88. https://doi.org/10.1016/0022-1694(93)90005-T.
Onda, Y., Tsujimura, M., Fujihara, J., Ito, J., 2006. Runoff generation mechanisms in high-relief mountainous watersheds with different underlying geology. J. Hydrol. 331, 659–673. https://doi.org/10.1016/j.jhydrol.2006.06.009.
Orlowski, N., Kraft, P., Pferdmenges, J., Breuer, L., 2016. Exploring water cycle dynamics by sampling multiple stable water isotope pools in a developed landscape in Germany. Hydrol. Earth Syst. Sci. 20, 3873–3894. https://doi.org/10.5194/hess-20-3873-2016.
Padrón, R.S., Wilcox, B.P., Crespo, P., Célleri, R., 2015. Rainfall in the Andean Páramo: New Insights from High-Resolution Monitoring in Southern Ecuador. J. Hydrometeorol. 16, 985–996. https://doi.org/10.1175/JHM-D-14-0135.1.
Pearce, A.J., Stewart, M.K., Sklash, M.G., 1986. Storm Runoff Generation in Humid Headwater Catchments: 1. Where Does the Water Come From? Water Resour. Res. 22, 1263–1272. https://doi.org/10.1029/WR022i008p01263.
Pellerin, B.A., Wollheim, W.M., Feng, X., Vörösmarty, C.J., 2008. The application of electrical conductivity as a tracer for hydrograph separation in urban catchments. Hydrol. Process. 22, 1810–1818. https://doi.org/10.1002/hyp.6786.
Pelletier, A., Andréassian, V., 2020. Hydrograph separation: An impartial parametrisation for an imperfect method. Hydrol. Earth Syst. Sci. 24, 1171–1187. https://doi.org/10.5194/HESS-24-1171-2020.
Penna, D., Stenni, B., Sanda, M., Wrede, S., Bogaard, T.A., Michelini, M., Fischer, B.M.C., Gobbi, A., Mantese, N., Zuecco, G., Borga, M., Bonazza, M., Sobotková, M., Čejková, B., Wassenaar, L.I., 2012. Technical note: Evaluation of between-sample memory effects in the analysis of δ2H and δ18O of water samples measured by laser spectroscopes. Hydrol. Earth Syst. Sci. 16, 3925–3933. https://doi.org/10.5194/hess-16-3925-2012.
Penna, D., van Meerveld, H.J., Oliviero, O., Zuecco, G., Assendelft, R.S., Dalla Fontana, G., Borga, M., 2015. Seasonal changes in runoff generation in a small forested mountain catchment. Hydrol. Process. 29, 2027–2042. https://doi.org/10.1002/hyp.10347.
Pesántez, J., Birkel, C., Gaona, G., Arciniega-Esparza, S., Murray, D.S., Mosquera, G.M., Célleri, R., Mora, E., Crespo, P., 2023. Spatially distributed tracer-aided modelling to explore DOC dynamics, hot spots and hot moments in a tropical mountain catchment. Hydrol. Process. 37, e15020.

Pinder, G.F., Jones, J.F., 1969. Determination of the ground-water component of peak discharge from the chemistry of total runoff. Water Resour. Res. 5, 438–445. https://doi.org/10.1029/WR005I002P00438.
Pionke, H.B., Gburek, W.J., Folmar, G.J., 1993. Quantifying stormflow components in a Pennsylvania watershed when 18O input and storm conditions vary. J. Hydrol. 148, 169–187. https://doi.org/10.1016/0022-1694(93)90258-B.
Quichimbo, P., Tenorio, G., Borja, P., Cárdenas, I., Crespo, P., Célleri, R., 2012. Efectos sobre las propiedades físicas y químicas de los suelos por el cambio de la cobertura vegetal y uso del suelo: Páramo de Quimsacocha al sur del Ecuador. Suelos Ecuatoriales 42, 138–153.
Ramón, J., Correa, A., Timbe, E., Mosquera, G.M., Mora, E., Crespo, P., 2021. Do mixing models with different input requirement yield similar streamflow source contributions? Case study: A tropical montane catchment. Hydrol. Process. 35, e14209.
Ribatet, M., Dutang, C., 2004. Generalized Pareto Distribution and Peaks Over Threshold.
Ribolzi, O., Vallès, V., Bariac, T., 1996. Comparison of Hydrograph Deconvolutions using Residual Alkalinity, Chloride, and Oxygen 18 as Hydrochemical Tracers. Water Resour. Res. 32, 1051–1059. https://doi.org/10.1029/95WR02967.
Rinderer, M., van Meerveld, H.J., McGlynn, B.L., 2019. From Points to Patterns: Using Groundwater Time Series Clustering to Investigate Subsurface Hydrological Connectivity and Runoff Source Area Dynamics. Water Resour. Res. 55, 5784–5806. https://doi.org/10.1029/2018WR023886.
Rodhe, A., 1987. The origin of streamwater traced by oxygen-18. Uppsala University.
Sahraei, A., Kraft, P., Windhorst, D., Breuer, L., 2020. High-Resolution, In Situ Monitoring of Stable Isotopes of Water Revealed Insight into Hydrological Response Behavior. Water 12, 565. https://doi.org/10.3390/w12020565.
Saraiva Okello, A.M.L., Uhlenbrook, S., Jewitt, G.P.W., Masih, I., Riddell, E.S., Van der Zaag, P., 2018. Hydrograph separation using tracers and digital filters to quantify runoff components in a semi-arid mesoscale catchment. Hydrol. Process. 32, 1334–1350. https://doi.org/10.1002/HYP.11491.
Segura, C., James, A.L., Lazzati, D., Roulet, N.T., 2012. Scaling relationships for event water contributions and transit times in small-forested catchments in Eastern Quebec. Water Resour. Res. 48, n/a-n/a. https://doi.org/10.1029/2012WR011890.
Seibert, J., McDonnell, J.J., 2002. On the dialog between experimentalist and modeler in catchment hydrology: Use of soft data for multicriteria model calibration, 23–1-23–14 Water Resour. Res. 38. https://doi.org/10.1029/2001WR000978.
Shope, C.L., 2016. Disentangling event-scale hydrologic flow partitioning in mountains of the Korean Peninsula under extreme precipitation. J. Hydrol. 538, 399–415. https://doi.org/10.1016/j.jhydrol.2016.04.050.
Sklash, M.G., Farvolden, R.N., 1979. The role of groundwater in storm runoff. J. Hydrol. 43, 45–65. https://doi.org/10.1016/0022-1694(79)90164-1.
Sklash, M.G., Stewart, M.K., Pearce, A.J., 1986. Storm Runoff Generation in Humid Headwater Catchments: 2. A Case Study of Hillslope and Low-Order Stream Response. Water Resour. Res. 22, 1273–1282. https://doi.org/10.1029/WR022I008P01273.
Smakhtin, V., 2001. Low flow hydrology: a review. J. Hydrol. 240, 147–186. https://doi.org/10.1016/S0022-1694(00)00340-1.
Smith, A., Welch, C., Stadnyk, T., 2016. Assessment of a lumped coupled flow-isotope model in data scarce Boreal catchments. Hydrol. Process. 30, 3871–3884. https://doi.org/10.1002/hyp.10835.
Soulsby, C., Piegat, K., Seibert, J., Tetzlaff, D., 2011. Catchment-scale estimates of flow path partitioning and water storage based on transit time and runoff modelling. Hydrol. Process. 25, 3960–3976. https://doi.org/10.1002/hyp.8324.
Soulsby, C., Birkel, C., Geris, J., Dick, J., Tunaley, C., Tetzlaff, D., 2015. Stream water age distributions controlled by storage dynamics and nonlinear hydrologic connectivity: Modeling with high-resolution isotope data. Water Resour. Res. 51, 7759–7776. https://doi.org/10.1002/2015WR017888.
Stadnyk, T.A., Delavau, C., Kouwen, N., Edwards, T.W.D., 2013. Towards hydrological model calibration and validation: simulation of stable water isotopes using the isoWATFLOOD model. Hydrol. Process. 27, 3791–3810. https://doi.org/10.1002/HYP.9695.
Stockinger, M.P., Bogena, H.R., Lücke, A., Diekkrüger, B., Cornelissen, T., Vereecken, H., 2016. Tracer sampling frequency influences estimates of young water fraction and streamwater transit time distribution. J. Hydrol. 541, 952–964. https://doi.org/10.1016/J.JHYDROL.2016.08.007.
Suecker, J.K., Ryan, J.N., Kendall, C., Jarrett, R.D., 2000. Determination of hydrologic pathways during snowmelt for alpine/subalpine basins, Rocky Mountain National Park. Colorado. Water Resour. Res. 36, 63–75. https://doi.org/10.1029/1999WR900296.
Tetzlaff, D., Uhlenbrook, S., Eppert, S., Soulsby, C., 2008. Does the incorporation of process conceptualization and tracer data improve the structure and performance of a simple rainfall-runoff model in a Scottish mesoscale catchment? Hydrol. Process. 22, 2461–2474. https://doi.org/10.1002/hyp.6841.
Tetzlaff, D., Birkel, C., Dick, J., Geris, J., Soulsby, C., 2014. Storage dynamics in hydropedological units control hillslope connectivity, runoff generation, and the evolution of catchment transit time distributions. Water Resour. Res. 50, 969–985. https://doi.org/10.1002/2013WR014147.
Tetzlaff, D., Buttle, J., Carey, S.K., McGuire, K., Laudon, H., Soulsby, C., 2015a. Tracer-based assessment of flow paths, storage and runoff generation in northern catchments: a review. Hydrol. Process. 29, 3475–3490. https://doi.org/10.1002/hyp.10412.
Tetzlaff, D., Buttle, J., Carey, S.K., van Huijgevoort, M.H.J., Laudon, H., McNamara, J.P., Mitchell, C.P.J., Spence, C., Gabor, R.S., Soulsby, C., 2015b. A preliminary assessment of water partitioning and ecohydrological coupling in northern headwaters using stable isotopes and conceptual runoff models. Hydrol. Process. 29, 5153–5173. https://doi.org/10.1002/hyp.10515.
Turner, J.V., Macpherson, D.K., Stokes, R.A., 1987. The mechanisms of catchment flow processes using natural variations in deuterium and oxygen-18. J. Hydrol. 94, 143–162. https://doi.org/10.1016/0022-1694(87)90037-0.
U.S. Bureau of Reclamation, 2001. Water Measurement Manual. Washington DC.
Vidon, P., Cuadra, P.E., 2010. Impact of precipitation characteristics on soil hydrology in tile-drained landscapes. Hydrol. Process. 24, 1821–1833. https://doi.org/10.1002/HYP.7627.
von Freyberg, J., Studer, B., Kirchner, J.W., 2017. A lab in the field: high-frequency analysis of water quality and stable isotopes in stream water and precipitation. Hydrol. Earth Syst. Sci. 21, 1721–1739. https://doi.org/10.5194/hess-21-1721-2017.
von Freyberg, J., Studer, B., Rinderer, M., Kirchner, J.W., 2018. Studying catchment storm response using event- and pre-event-water volumes as fractions of precipitation rather than discharge. Hydrol. Earth Syst. Sci. 22, 5847–5865. https://doi.org/10.5194/hess-22-5847-2018.
Wang, L., von Freyberg, J., van Meerveld, I., Seibert, J., Kirchner, J.W., 2019. What is the best time to take stream isotope samples for event-based model calibration? J. Hydrol. 577, 123950 https://doi.org/10.1016/J.JHYDROL.2019.123950.
Weiler, M., McDonnell, J.J., Meerveld, I.T., Uchida, T., 2005. Subsurface Stormflow. Encycl. Hydrol. Sci. 10.1002/0470848944.HSA119.
Wen, H., Brantley, S.L., Davis, K.J., Duncan, J.M., Li, L., 2021. The Limits of Homogenization: What Hydrological Dynamics can a Simple Model Represent at the Catchment Scale? Water Resour. e2020WR029528 Res. 57. https://doi.org/10.1029/2020WR029528.
Willems, P., 2009. A time series tool to support the multi-criteria performance evaluation of rainfall-runoff models. Environ. Model. Softw. 24, 311–321. https://doi.org/10.1016/J.ENVSOFT.2008.09.005.
Zhiña, D.X., Mosquera, G.M., Esquivel-Hernández, G., Córdova, M., Sánchez-Murillo, R., Orellana-Alvear, J., Crespo, P., 2022. Hydrometeorological Factors Controlling the Stable Isotopic Composition of Precipitation in the Highlands of South Ecuador. J. Hydrometeorol. 23, 1059–1074. https://doi.org/10.1175/JHM-D-21-0180.1.
Zuñiga, V., 2018. Evaluación Geomecánica de la rampa de acceso del yacimiento Loma Larga. Universidad Central del Ecuador.